POLITECNICO DI TORINO

Master's Degree in Mechatronic Engineering

Design and Analysis of a Bio-Inspired Caudal Fin Using Shape Memory Alloys

THIS THESIS WAS CONDUCTED IN COLLABORATION WITH CAR
UNIVERSIDAD POLITECNICA DE MADRID

UPM
UNIVERSIDAD POLITECNICA DE MADRID

Supervisors:
Chiaberge Marcello
Claudio Rossi

Candidate:
Donato Rinaldi

Academic Year 2024/2025

Abstract

Over the years, bio-inspired robotics has become of particular relevance, especially with the construction of systems capable of reproducing a fluid and noiseless motion, capable also of exploring and monitoring the marine environment.

This work aims to model and realize an active biomimetic caudal fin, which guaranties the generation of a controllable movement through the utilization of SMA (Shape Memory Alloy) wires. The main objectives of this research are to design and develop a soft robotic structure capable of emulating the kinematic behavior of real caudal fins of fish. The study focuses mainly on deformation and actuation performance and to demonstrate the efficiency of using SMA as actuators for underwater use.

After an accurate study of the State of the Art, aimed at understanding the kinematics and mechanism of the generation of water jets and vortices of fishes, a simplified model of the caudal fin motion was developed, focusing on the deformation profile and the dynamic response achievable through SMA actuation.

To record the effects of body imbalance and to verify the contribution of the fin to pitch stabilization, an IMU sensor was integrated into the system.

Tests highlighted that the fin was capable of reproducing regular and symmetric deformations, with a dynamic response similar to the natural movements of small fishes.

The results showed that this biomimetic approach, associated to the use of smart and soft actuators, was extremely valid, showing the potential development of robotic fishes, capable of active control and to generate forces that allow 3D maneuvering in marine environment.

Quantitative analyses confirmed the repeatability and symmetry of the motion, validating the efficiency of the actuation system and the reliability of the silicone-based structure under multiple test cycles. Moreover, the obtained data prove the feasibility of the fin driven by SMA wires, adding advantages, such as lightweight, silent and adaptable system for future bio-inspired robotic applications.

Contents

1 State of the Art 5

1.1 Bio-inspired Underwater Robots 5

1.1.1 Introduction 5

1.1.2 Historical Background 6

1.1.3 Swimming Modes and Morphology 7

1.2 Smart Actuators for Soft Robotics 9

1.2.1 EAP (ElectroActive Polymers) 9

1.2.2 PZT (Piezoelectric Actuators) 10

1.2.3 FEA (Fluidic Elastomer Actuators) 10

1.3 Shape Memory Alloys (SMA) 11

1.4 Control of the SMA 13

1.4.1 Morphology and dynamics of the fins 14

1.4.2 Pitching stabilization 16

2 Fish Robot Design 18

2.1 System Overview 18

2.2 Mechanical Design 18

2.3 Prototype Assembly 20

2.4 Fin Geometry and Deformation Analysis 22

2.5 Assembly Challenges and Improvements 23

3 Electronics and Control System 24

3.1 Electronic system 24

3.2 First PCB Version 25

3.2.1 Objective of the First PCB 25

3.2.2 Structure of the actuation channel 26

3.2.3 First Problem: drop voltage too small 26

3.2.4 Second Problem: dissipation on the sense resistor 27

3.2.5 Third Problem: pin assignment and start of the microcontroller . . 27

3.3 New PCB Version 28

3.3.1 New value for the sense resistor R_5 28

3.3.2 Simplification of the measurements 29

3.3.3 Pins reassignment and multi-board . . . 29
3.4 Software Implementation . . . 30
3.4.1 Protections and safety measures . . . 31
3.5 User Interface . . . 32
3.6 Preliminary Tests . . . 34
3.6.1 Test on a single channel . . . 34
3.6.2 Test on multiple channels/multi-board . . . 34
3.6.3 IMU Validation . . . 34

4 Sensors and Measurement Setup . . . 35
4.1 Hardware IMU Integration . . . 35
4.2 Data Acquisition . . . 37
4.3 Experimental methodology . . . 37

5 Static Calibration . . . 39
5.1 Test bench and Instrumentation . . . 39
5.1.1 Test Protocols . . . 40
5.1.2 Data Acquisition and Processing . . . 40
5.1.3 Uncertainty and Repeatability . . . 42
5.2 Relation between Current, Resistance and Deflection Angle . . . 42
5.2.1 Electrical characterization of the SMA (current–resistance) . . . 42
5.2.2 Static calibration: resistance vs. deflection angle . . . 43
5.2.3 Inverse model: angle estimation from resistance . . . 44
5.3 Preliminary PID controller design . . . 45
5.3.1 Initial Model . . . 45
5.3.2 Procedure with MATLAB . . . 46
5.3.3 Simulation Results . . . 47
5.4 Results and Discussion . . . 49
5.4.1 Qualitative analysis of the fin motion . . . 49
5.4.2 Quantitative analysis of calibration results . . . 49
5.4.3 Limitations on the design PID controller . . . 50

6 Effects of the Caudal Fin in the Pitching Stabilization . . . 51
6.1 Experimental setup . . . 52
6.1.1 Mechanical Structure and Prototype Assembly . . . 52
6.1.2 Control Interface . . . 52
6.1.3 Sensors and Data Acquisition . . . 53
6.2 Experiments and Procedures . . . 54
6.2.1 Strategy for Experiments . . . 54
6.2.2 Procedure and Data Collection . . . 54

6.3 Actuation Configurations and Trials 54
6.3.1 Mode 0 - S-movement 55
6.3.2 Mode 1 - All the SMA 56
6.3.3 Mode 2 - TOP (only superior half) 57
6.3.4 Mode 3 - BOTTOM (only inferior half) 57
6.4 Results and Discussion 58

7 Conclusions and Future Work 60
7.1 Summary of Achievements 60
7.2 Prototype Limitations 61
7.3 Future Developments 62
7.4 Sustainability and UN 2030 Agenda 63

Bibliography 66

List of Figures

1.1 Forces acting on the fish 6
1.2 BCF modes 7
1.3 SMA's Hysteresis and non-Linearity 12
1.4 Difference of position between COM and COB 14
1.5 Movement of fins of the fish 15

2.3 Previous Caudal Fin with two SMA wires with M-shaped 21
2.4 Final Caudal Fin with four SMA wires 22

3.1 First PCB Version 27
3.2 New Version of the PCB 28
3.3 Electronic inside the case 30
3.4 Flowchart of the control and data acquisition logic implemented on the ESP32-S3. 33

4.1 IMU Adafruit BNO055 used for the study 36

5.1 Deflection angle measured through Tracker 40
5.2 Resistance evolution and plateau region – DAC = 3000 41
5.3 Angle-Resistance Relation and Linear Fit 44
5.4 Step-response of the system with no controller applied 46

5.5 PID controller for simulations 47
5.6 Step-response of the system with an aggressive PID controller applied . . . 48
5.7 Comparison between the two systems: in blue the original one and in red the controlled one 48

6.1 Whole setup of the prototype 52

7.1 Life Below Water of the UN 2030 Agenda 64

List of Tables

2.1 List of materials used for the fabrication of the caudal fin. 19

3.1 Functional structure of the electronic control system 25
3.2 Organization of the modules of the firmware 31

5.1 Mean resistance, deflection angle and steady-state SMA resistance for each DAC level 43
5.2 Raw deflection angle measurements for each DAC value 44

6.1 Used parameters for each trial in Mode 0 (S-movement) 55
6.2 IMU Results for Mode 0 (S-movement) 55
6.3 Used parameters for each trial in Mode 1 (All the SMA) 56
6.4 IMU Results for Mode 1 (All the SMA) 56
6.5 Used parameters for each trial in Mode 2 (TOP - Superior Half) 57
6.6 IMU Results for Mode 2 (Superior Half) 57
6.7 Used parameters for each trial in Mode 3 (BOTTOM - Inferior Half) . . . 58
6.8 IMU Results for Mode 3 (Inferior Half) 58

Chapter 1

State of the Art

1.1 Bio-inspired Underwater Robots

1.1.1 Introduction

For decades, the large and costly demand for underwater vehicles (especially robots) has been crucial for the numerous missions, increasing progressively the use of these vehicles. Consequently, over the years, these have been studied and improved in efficient terms, for example:

- the substitution of locomotive-efficient vehicles with conventional propelled ones
- Propelling actuators have been replaced with electric rotatory actuators due to the better precision and keeping torque magnitudes overtime. In addition, propelling actuators are rigid and considerable energy consumption devices (adding mass, inertia and friction to the mechanical system), noisy and prone to harm subaquatic flora and fauna

The better idea is to use bioinspired robotic fishes owing to better quality to swim, that depends mostly on the type of fish's shape, skeletal structure for mobility and hydrodynamic motion waves performed for propulsion and maneuverability. Another extremely important focus on the design of fish is the calculus and involvement of inner and external forces in the hydrodynamic locomotion process. The most significant ones are drag and thrust apply horizontally, while lift, buoyancy and weight apply vertically. Through the use of roll-pitch-yaw Euler angles, the hydrodynamic steady angular orientation motions are analyzed. There are elements of the fish which are propulsive elements, such as fins and musculoskeletal parts. These are capable of exerting hydrodynamic forces and producing linear and angular momentum during a locomotive interaction with the water surrounding it, as shown in Figure 1.1.

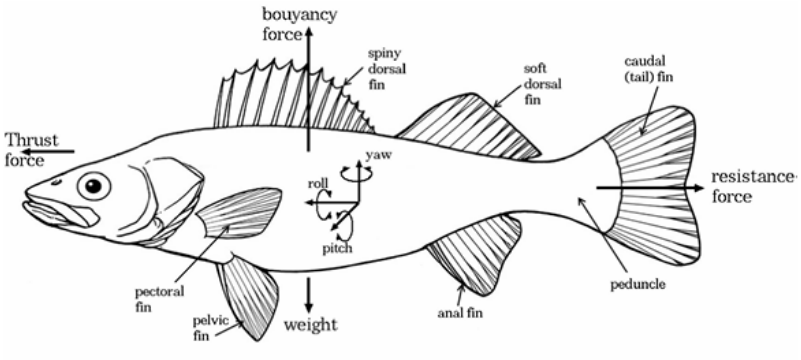

Figure 1.1: Forces acting on the fish

Fish locomotion is based on morphological and biomechanical modifications that enable undulatory swimming. By transmitting momentum to the surrounding water through drag forces, fish can either maintain steady cruising speeds or produce lift and acceleration, depending on hydrodynamic balance. Their body shape and the way their skin interacts with the water affect drag, lift, and flow patterns. These traits allow fish to move swiftly and efficiently and swim in several ways, such as gliding, jet propulsion, burrowing, jumping, and even flying.

1.1.2 Historical Background

Bionics is a discipline which investigates the structural and functional characteristics of organisms to reproduce tool based on these principles. The most fascinating and interesting environment on Earth is the ocean, since it occupies two-thirds of it and most of it is unexplored. The attention in was especially from engineers and researchers, who see this as a challenge, for many reasons, such as the large size, the low energy conversion efficiency and poor mobility of existing underwater detection and operation devices. To overcome all these obstacles, the researchers have come up with the idea of robotic fish (inspired by the various fishes which have evolved over millions of years) which is a new type of autonomous underwater vehicle (AUV) that integrates hydrodynamics, machinery, electronics, control and computer technologies. They are used for numerous applications, including marine observation, environmental protection and rescue operations, and each of these must encounter specific requirements. It is not a research project of the last years, since the first research about it can be tracked in 1926 when Breder classified the swimming modes of fish in two categories: body and/or caudal fin swimming (BCF) and median and/or paired fin swimming (MPF). Then another experiment on the observation of the dolphins was made in 1936, but the real breakthrough in this field was made in 1960s where there were theoretical studies that lead to two types of theories with the forces: resistive force theory (which explained better the viscous force) and reactive force theory (which explained in a more accurate way the inertia). In the

following years, the most effective ones were the reactive force theories, and three theories were proposed and used for hydrodynamic modelling: the elongated body theory (EBT) proposed by Lighthill in 1970, the actuator disc theory proposed by Horlock in 1978, and the wave plate theory (WPT) proposed by Cheng in 1994. In 1995, at the Massachusetts Institute of Technology (MIT), there were some prototypes of bionic robotic fish with the Robo Tuna and Robo Pike developed. From that moment, several studies and researches were conducted in the field, until nowadays where the main objective is to optimize the system in all the way possible, so in the mechanical design (using smart materials and actuators, and compliant mechanisms), but also in the control strategies (improving the robotic performance, and designing closed-loop control based on onboard sensors to a more accurate and precise control). With the development of mechatronic system, the robotic fish has almost entirely substituted the conventional underwater vehicles, since they overcome shortcomings, such as the large scale, low energy efficiency and disturbance to the environment. In addition, these new vehicles are characterized by a great superiority in propulsive efficiency, maneuverability and stealth, hence they are used for several underwater missions, mainly explorations, rescues, samplings and water quality monitoring.

1.1.3 Swimming Modes and Morphology

Returning to the categorization made initially the BCF mode can be classified into anguilliform, subcarangiform, carangiform, thunniform, andostraciiform, while the MPF mode into rajiform, diodontiform, labriform, amiiform, gymnotiform, balistiform and tetraodontiform. In this study, the main focus will be on the BCF mode. In FIgure 1.2, all BCF modes are shown.

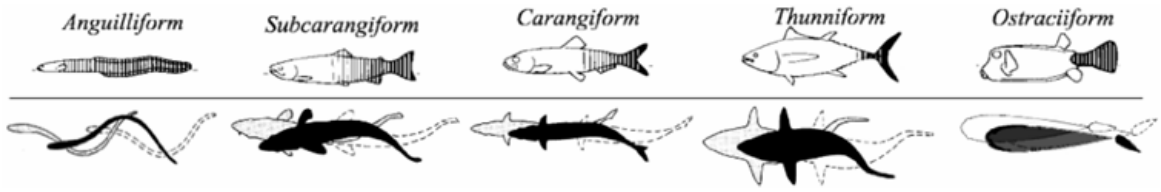

Figure 1.2: BCF modes

In anguilliform mode, the swimming is based on axial waves propagating in the whole body (from head to tail) with a number of waves equal to one body length. Robots inspired by this mode are usually characterized by high maneuverability, obtained with a hyper-redundant design. There are different kinds of projecting this, for example Bayat et al. developed six active modules, a passive flexible tail and an un-actuated head module, while Struebig et al. made the core component of the robot as a helix, abandoning the idea of hyper-redundant design. The last one is interesting because they powered it with a

single DC motor installed on the head, which made the robot more efficient with a simply control strategy, but the large scale and lack of waterproof measures of each element made a larger friction force in swimming.

While the undulation is made for the whole body in anguilliform mode, for subcarangiform and carangiform is confined in the posterior part of the robotic fish, with the anterior part almost rigid. At the expense of lower maneuverability respect the previous case, these two modes are higher in speed.

The thunniform mode has a crescent-shaped caudal fin and while the fish is swimming and the tail is moving, the whole body remains rigid, achieving high speed and efficiency.

But the most stable mode is the ostraciiform, since the undulation involved the least number of body parts. They are characterized by a large scale and inefficient fin actuation, that leads to a low speed, but they can maneuver in a narrow space through the fin actuation. Costa et al. proposed a robotic fish in this mode with a cylindrical rigid body and a tail section, powered by a DC brushed motor to convert the continuous rotation of the drive into a harmonic oscillation. Zhang et al. presented a robot with a 2-segment caudal. To gain stability, a large and heavy main body was projected, while the caudal fin is actuated by an electromagnetic actuator to obtain higher frequency oscillations (over 50 Hz).

The one of interest is the carangiform swimmer robots because the caudal fin is moving, while the whole body is basically rigid and inflexible. They oscillate dorsal, pectoral and caudal fins to balance, maneuver and control hydrodynamic movements. It is the preferable mechanism to use it in this case for the following reasons:

- needing at least one active joint, so low amount of energy consumption and it classifies them as the least energy spending system
- highest flexibility
- simplest mechanical complexity
- smoothest locomotion mode
- reduced in terms of physical space requirements
- does not require a tail bending

This mechanism of movement has been implemented in various ways: using macro fiber composite (MFC), piezoelectric composite (PZC), polyethylene terephthalate (PET) and shape memory alloys (SMA).

1.2 Smart Actuators for Soft Robotics

Since the beginning of the construction of robotic fishes, traditional motors were used, even with the shortcomings that came up with, such as the heaviness, since there are several parts of which the motor is made, and the generation of noises and disturbances that did not make possible the utilization of these in practical missions. The advent of new technologies like artificial muscle-based actuators was crucial. Even if they are not so accurate and powerful as the traditional motors, these smart actuators provide high deformability and adaptability due to their excellent compliance. The most used in this field are shape memory alloy (SMA), electroactive polymer (EAP), piezoelectric actuators (PZT), and fluid elastomer actuator (FEA).

Focusing on the method with SMA, they are based in multiple serially connected springs to emulate damping muscles. The SMA has been mechanically deformed and then returned to their original shape once heated at a certain temperature. The lateral SMA wires overlaid an elastic substrate (in the middle) that provides mechanical resistance and stores elastic energy. Therefore, the caudal fin is a noiseless actuation compliant device yaw bending.

Between electrical properties polymers, pneumatic and hydraulic control devices, the electrical ones are the most used due to their small size and reduced energy costs. It is also preferred an underactuated mechanism because of the reduced number of active joints and for the most realistic biological swimming behaviors. In the near future, the addition of novel artificial tendons and muscles in the robotic fishes will provide them with better properties, especially behaving like biological muscles and with augmented mechanical power, reduced weight and volume, efficient linear extension/contractile motions electrically commuted.

Nowadays soft material technology is used in robot fishes providing suitability to perform efficient swimming maneuverability and they are comprised of complex dynamic control models.

1.2.1 EAP (ElectroActive Polymers)

Many types of smart actuators have been studied for robotic fish, especially those based on ElectroActive Polymers (EAPs). EAPs can be divided into two main categories:

- Ionic EAPs (IPMC, PPy): Ionic Polymer-Metal Composites (IPMC) deform through ion redistribution under a low applied voltage (1–3 V), when an electric field is applied. Perfect in applications that want to provide small bending stress. Their main use is in small-scale robotic fish (length < 100 mm). Similarly, Polypyrrole (PPy) actuators are fabricated with conductive polymers, but, in addition, they produce bending motion under small voltages. They are widely used in this field due to their

low cost, good conductivity, and fast response

- Electronic EAPs (Dielectric Elastomers, DE): When a high voltage (over 1 kV) is applied, these generate Maxwell stress between electrodes, leading to membrane expansion. DE actuators can achieve very fast response times (less than 200 micros) and very large actuation strains (over 100%), making them a better alternative for fish-like propulsion, although the high driving voltage is a limitation

1.2.2 PZT (Piezoelectric Actuators)

Another type of smart actuator used in robotic fish is based on piezoelectric ceramics (PZT), which operate through the inverse piezoelectric effect and deform when electrically excited. PZT actuators are characterized by high driving stress (about 110 MPa) and fast frequency response, but they suffer from very small strain (about 0.2%), meaning that displacement amplification mechanisms are usually required. Several designs have been proposed:

- Early works used THUNDER (THin-layer composite UNimorph ferro electric DrivER and sensor) actuators directly connected to the tail fin, but their size made the robotic fish bulky
- LIPCA (lightweight piezocomposite actuator) actuators were developed as a lighter alternative, but still required mechanical systems (e.g., rack-and-pinion or multilayer magnifying mechanisms) to increase displacement
- Miniaturized robotic fish have also been achieved, such as a 1.93 g fish actuated by PZT bimorph cantilevers with a four-bar linkage, capable of reaching speeds around 4.5 cm/s

Overall, PZT actuators provide fast and powerful actuation, but their limited strain and need for magnification systems restrict their direct application in compact robotic fish designs.

1.2.3 FEA (Fluidic Elastomer Actuators)

Another category of actuators used are Fluidic Elastomer Actuators (FEA), distributed in the whole body, which make the robot soft and compliant. These actuators are built from super-elastic materials with chambers that expand under pressurized gas or liquid, producing bending or stretching motions. Two types of actuators are involved here:

- Pneumatic actuators use compressed gas; for example, robotic fish have been built with pneumatic layers and onboard gas regulation to achieve escape maneuvers with large heading angles (up to 100°). However, challenges include limited endurance due to power supply constraints and buoyancy control issues caused by gas release

- Hydraulic actuators can use the surrounding water in a closed cycle, which allows faster response and larger force compared to pneumatics

Overall, FEAs provide high compliance and biomimetic motion, but practical issues with power and buoyancy remain for underwater applications.

1.3 Shape Memory Alloys (SMA)

Various actuators have been tested for these kinds of applications and through all of the studies, it turned out that SMA (Shape Memory Alloys), IPMC (Ionic Polymer Metal Composites) or hybrid actuator-driven robots are more compact and move faster than PZT (piezoelectric) robots. On this study, the focus is on the SMA actuators.

Shape memory alloy (SMA) is influenced by both temperature and internal stress, exhibiting thermodynamic characteristics and the shape memory effect (SME) under specific conditions. The wires made of SMA can be stretched when cool and when they heated, they will contract forcefully, for this reason nowadays there is a large use of them as actuators.

The austenite phase transforms into the twinned martensite phase upon cooling and then into the detwinned martensite phase upon application of stress, constituting a positive transformation. Upon heating the martensite phase, the forward transformation deformation is reversed, leading the material to return to its original shape (inverse transformation). The phase transformation is non-linear and exhibits large thermal hysteresis.

There are two main types of shape memory effect:

- One-way shape memory effect, where at the martensite phase, an external force is applied to stretch the alloy, until the force is removed, where, from that moment, the alloy shows permanent deformation. It can recover its original shape upon heating. Subsequent cooling does not change shape unless it is stressed again

- Two-way shape memory effect, which is basically the same thing as before, expect that here the shape change occurs upon cooling and without the applying of external stress. The SMA usually needs to be trained to exhibit the two-way effect

Heating the SMA actuators can be done by feeding them with electrical current and so applying the Joule effect.

The actuation speed of SMA wires depends on both heating and cooling rates. Since thin nitinol wires cool faster than they heat under standard operating currents, faster actuation can be achieved by applying higher-than-recommended currents, according to the technical data sheets for nitinol wires. However, overheating the wires causes excessive temperatures, which slow cooling and risks thermal degradation. Kuribayashi (1991) addressed this issue by regulating current through direct temperature monitoring with a

thermocouple: high current is applied only when the wire is below a set threshold. A similar rapid-heating approach eliminates the temperature sensor by estimating temperature indirectly through electrical resistance.

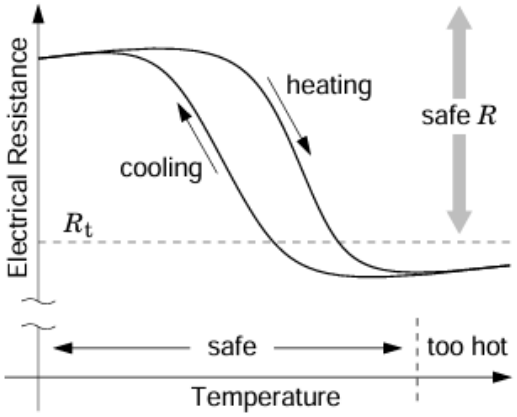

Figure 1.3: SMA's Hysteresis and non-Linearity

As shown in Figure 1.3, because of hysteresis in the temperature-resistance relationship, the exact wire temperature cannot be determined from resistance measurements. However, a threshold resistance (R_t) can be defined such that, if the measured resistance exceeds this value, the wire is guaranteed not to be overheated. In practice, a safety margin must be included in the choice of Rt to account for measurement uncertainty and resistance variations due to strain.

They are used for applications which require high levels of stress (up to 200 MPa) with low voltage (approximately 2 V), making it a suitable actuator. The aquatic environment is suitable for cooling SMA and achieving higher frequency.

SMA actuators offer advantages such as low cost, simple structure, high stress and strain capacity, and corrosion resistance. They are largely used for flexible and miniaturized force control applications due to their high force-to-weight ratio, mechanical simplicity, compactness, as well as silent, clean operation. However, their recoverable strain is limited (4–8%). When configured as springs, the strain amplitude increases significantly (200–1000%), but at the expense of stress generation, restricting their use to small robotic fish. Moreover, energy inefficiency, slow speed and inaccurate response are significant disadvantages for these kinds of actuators. Another major limitation is the need for rapid temperature variation, which makes the control more difficult and prevents SMA-driven robotic fish from achieving full autonomy. Despite all, SMA technology is the most appropriate one for the application in ocean engineering, due to the weight, volume, structure and output force.

Recent studies have shown that shape memory alloys (SMA) can effectively drive bionic fish propulsion systems, enabling flexible, lifelike movements.

In 2019, Li et al. developed a crucian carp-inspired fishtail that achieved a final propulsion frequency of 0.8 Hz oscillation, a bending angle of 22° and 0.041 N of average propulsion force, with a heating time of 80 ms.

In 2018, William et al. created a black bass-inspired robotic fish with SMA linear actuation, demonstrating superior efficiency and performance (with a faster response than the other one), but limited by actuator fatigue.

In 2021, Muralidharan et al. designed a 3D-printed subcarangiform AUV with NiTi SMA springs, reaching a maximum swing angle in aqueous environment of 50° and 24.5 mm/s forward velocity, though the use of an external power supply.

1.4 Control of the SMA

Due to the non-linearity of the SMA, it is more appropriate a non-linear control, mostly because of the hysteresis of the SMA. Non-linear control, like fuzzy logic, can keep track of this phenomenon, but also compensate for dynamic delays, reduce tracking errors when the current rapidly change and it can guarantee more precision and stability. So, these kinds of controls can describe better the real behavior of SMA.

However, non-linear control is expensive in time and production of it. In addition, the interval where the SMA is used is an interval that can be linearized around the operating point, obtaining an equivalent linear model. In this case of study, moderate operating speeds and the absence of extreme precision requirements allow the design of a linear control strategy that can still provide acceptable performance.

The PID is an optimal solution to this problem. The PID (Proportional Integrative Derivate) computes the past, present and future control and it is the most applied linear control because both transient response and steady state response are improved. The idea of this control is to control the error before the error develops. A very small derivate gain is necessary because this gain interacts with the response, making it very sensible to the noise in the process variable signal and, consequently, the control system unstable and the response very slow.

The PID controller can be written in the following way:

$$u(t) = K_p + K_i \int_0^t e(\tau)\, d\tau + K_d \frac{de(t)}{dt}$$

Where:

- $u(t)$ is the control signal
- $e(t)$ is the error, which is the difference between a reference and the actual measurement

- K_p, K_d and K_i are the gains, respectively the proportional, derivative and integrative gain.

An interesting approach used in this case of study is the Ziegler-Nichols Step Response Method, which is based on a registration of the open loop step response of the stable system. In this method, the unit-step response curve should look like S-shaped, which is characterized by two parameters, which are delay time L and time constant T. For the parameters of the PID, the following formulas are used:

$$K_d = \frac{1.2}{a} \qquad T_i = 2 * L \qquad T_d = \frac{L}{2}$$

Where $a = \frac{KL}{T}$, so the formulas will be adjusted in the MATLAB script where all the calculations are made.

1.4.1 Morphology and dynamics of the fins

The postural stability of fish while it is swimming and, particularly, during the hovering or maneuvering at low speed, is one of the challenges to make a robotic fish more like a real fish. A key aspect is the relationship between the center of mass (COM) and the center of buoyancy (COB) because, in most cases, they do not coincide. The first one is positioned in the dorsal part of the fish and is determined by the distribution of major muscle groups and the axial skeleton, while the second one is situated ventrally and is determined by the location of the viscera and swim bladder. So, they are positioned in two different parts of the fish and this separation between them, inevitably, generates torque around the center of mass, making the fish roll and pitch involuntarily, constantly making the fish adjust it by itself. The Figure 1.4 shows this phenomenon.

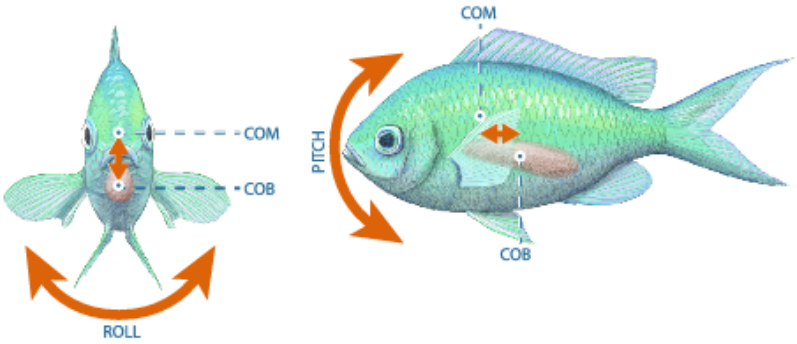

Figure 1.4: Difference of position between COM and COB

This instability condition is particularly relevant in near-neutrally buoyant fishes, for which even little internal perturbations, like branchial ventilation, or external perturbations, like flow turbulences, generate rotations around the COM. The result is that the

balance in a certain stationary position is not energetically neutral: fishes must rely on active fin control, increasing twice the resting levels. The analysis demonstrates that a greater distance between the COM and the COB and with more intense caudal fin activity, leads to higher energetic costs. On the other hand, fishes with pectoral fins positioned more posteriorly relative to the COM can exploit a greater lever arm, which results in an improvement of the efficiency of postural corrections and reduction of energetic costs.

The various fins perform complementary functions. The pectoral fins can produce corrective moments through small oscillatory movements. Their anatomic position is decisive because they are located near the COM, which provides a shorter lever arm, leading to lower stabilizing effectiveness; different dynamic for fins located further back, allowing more efficient control with relatively modest forces. On the other hand, the caudal fin is not solely responsible for thrust generation. According to functional morphology and hydrodynamic studies, the purpose of the caudal fin is to maintain the balance of the body of the fish, especially during unstable maneuvers such as the backward swimming or the forward sinking. To make these movements, the caudal fin can modulate its kinematics, for example producing fluid jets that generate compensatory moments. These forces are crucial because they can contrast the destabilizing effects produced by the separation of the two centers, stabilizing pitch and preventing undesired rotations.

To sum up, the interaction between caudal and pectoral fins is determinative for stabilization because the first one contributes to the thrust and the generation of moments that correct longitudinal imbalances, while the other ones provide a localized control capable of damping rotations and maintaining the desired posture. This dynamic equilibrium is expensive in terms of energetic costs, growing with the distance between COM and COB and with intensified caudal fin activity. Therefore, in the end, fish stability is never a passive condition, and the fish locomotion is characterized by a constant tension between morphological instability and active stabilization.

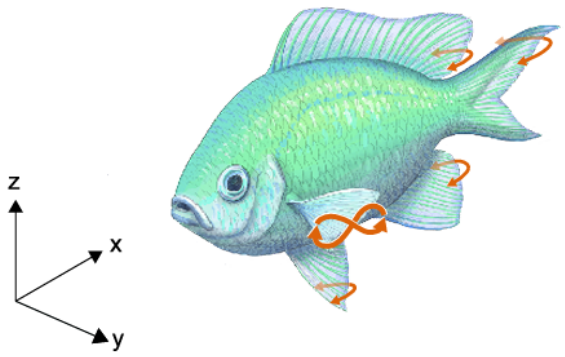

Figure 1.5: Movement of fins of the fish

1.4.2 Pitching stabilization

A significant contribution to the comprehension of the dynamic of the caudal fin is its function of stabilization, studied by Flammang and Lauder (2008), which analyzed in detail the phenomenon of caudal-fin propagation (CFP), that is the propagation of a wave on the caudal fin during low velocity swimming. Their purpose is to prove that this movement contributes to the propulsion and to the pitching stabilization in inherently unstable postures.

They use a stereoscopic digital particle image velocimetry (SDPIV) to visualize the three-dimensional velocity fields in the wake of the caudal fin and pectoral fins. By operating with a vortex-ring impulse model, they obtained hydrodynamic forces, meanwhile other quantitative data were estimated, such as body kinematics, body inclination and tail-beat frequency. The results derived that, during forward sinking (a maneuver in which the fish descends head-down), the CFP generates a series of posterodorsally oriented jets. Focusing exclusively on the caudal fin, it experiences a small propulsive force and a vertical downward force (negative lift) acting posterior to the center of mass. This is crucial since this vertical component induces a nose-up pitching moment, counteracting destabilizing torques caused by the relative positions of the center of mass and the center of buoyancy. Other factors that were measured are the forces, seeing that they were small (on the order of millinewtons), with the vertical component which prevails over the longitudinal one, highlighting that the primary role of the CFP is stabilization rather than propulsion.

Another confirmation of the study is the destabilizing effect of the pectoral fins during specific phases. For example, during the down-stroke, the pectoral fins produce a jet that creates a nose-down pitching moment, opposite to the stabilizing effect of the caudal fin. On the other hand, during up-stroke, the jet is more aligned with the longitudinal axis, contributing mainly to thrust with minimal influence on pitch.

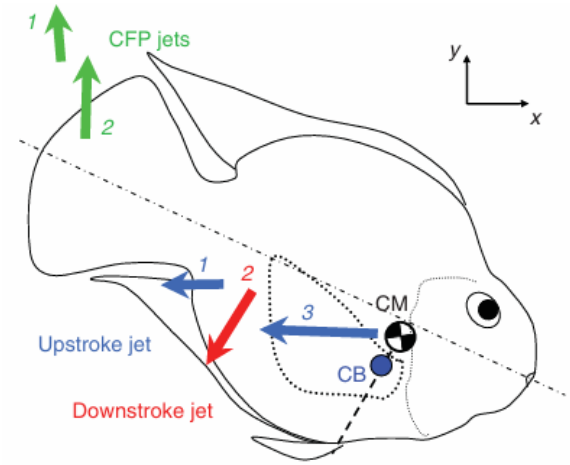

This is a dynamic balance of moments, in which the caudal fin compensates for desta-

bilizing torques arising both from hydrodynamic interactions and from hydrostatic imbalances linked to separation of center of mass and center of buoyancy.

According to morphological examination, when the fish acquires an inclined posture, the center of buoyancy of the species under study is located slightly posterior to the center of mass. To maintain a stable orientation, active fin movements must offset the hydrostatic nose-down moment created by this design. The CFP accomplishes precisely this: an upward-directed wave that travels from the ventral to the dorsal region of the caudal fin generates fluid jets that provide an opposing nose-up moment, stabilizing the body pitch.

By doing this, the caudal fin maintains stability during hovering and slow-descent maneuvers by counteracting the torque generated by buoyancy as well as the destabilizing influence of the pectoral fins.

Chapter 2

Fish Robot Design

2.1 System Overview

The purpose of the experimental phase is the realization of an active caudal fin that simulates the real one of a fish, paying particular attention to this process, since from this depends on the reproduction of a realistic and controllable movement. So, the first part of this project is the realization of this caudal fin, activated by SMA wires and integrated into a rigid body, to analyze the generated forces and the eventual body imbalance through inertial sensors (IMU). In this whole phase, an interactive experimental approach was adopted: the three-dimensional modeling, mold fabrication, silicone casting, and subsequent manual refinements.

2.2 Mechanical Design

The fin was designed in CAD model and printed with an Anycubic Photon Mono X, a printer based on SLA (Stereolithography) technology, which made sure to get a smooth surface and precise details, to obtain clean silicone castings and facilitate demolding. The final geometry follows a fan-like shape, with a broader base and a thinner free edge, allowing for gradual deformation of the flexible material during actuation, inspired by the morphology and flexibility distribution typical of carangiform fish tails.

The 3D model was designed according to the requirements of resin-based additive manufacturing, such as:

- adding small draft angles to facilitate demolding
- rounding sharp edges to prevent stress accumulation within the silicone

The printing material utilized was a rigid photopolymer resin, which has better mechanical resistance to the temperature and pressure of liquid silicone.

After molding, the piece was cleaned with isopropyl alcohol (IPA), to take off the residuals of the resin, and then submitted to UV post-care (for about 5 minutes), lightly sanded and treated with a release agent to facilitate the silicon's pouring. At the end, a PVA based release agent was applied to prevent adhesion of the silicone and to ensure easy removal of the cured component.

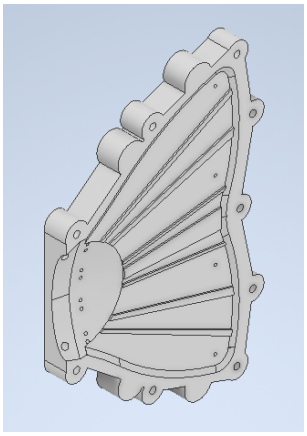

(a) CAD of the fin

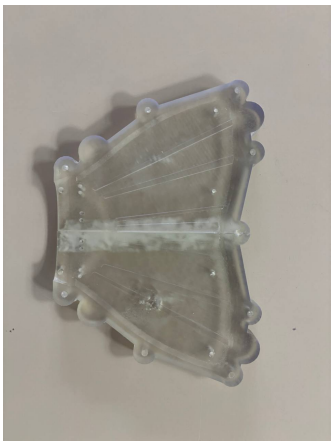

(b) Fin after printing and cleaning

Table 2.1: List of materials used for the fabrication of the caudal fin.

Material	**Function**	**Reason for choice**
Platsil Gel-25 (Part A + Part B)	Flexible fin membrane	Platinum-cure silicone with very low Shore hardness (00–25), providing high elasticity, transparency, and excellent waterproofing. Used for casting the entire fin body.
Pol-Ease 2500 Release Agent	Mold release agent	Applied to the 3D-printed mold to prevent adhesion of the silicone and facilitate clean demolding without damaging the printed surface.
Rigid photopolymer resin	3D mold	High precision and dimensional stability during silicone casting and curing process.
Nitinol (SMA wire Ø150 mm)	Actuator	High force-to-weight ratio and reversible deformation when electrically heated, ensuring smooth and controllable fin bending.
Resin pins	SMA alignment	Provides mechanical stability and correct positioning of the SMA wires within the mold during silicone pouring.

2.3 Prototype Assembly

Once the mold was prepared, custom pins were inserted into the dedicated alignment holes and their purpose is to support the SMA wires during the casting process, providing the precise positioning and the right tension of the wires. The geometry of the pins is simple, but two aspects were important during the design:

- a small upper groove, which guarantees the right positioning of the wires and prevents lateral slipping during casting
- a wider lower base, solely to prevent the pin from entering too deeply into the mold cavity

The height of the pin was chosen, avoiding contact with the mold surface.

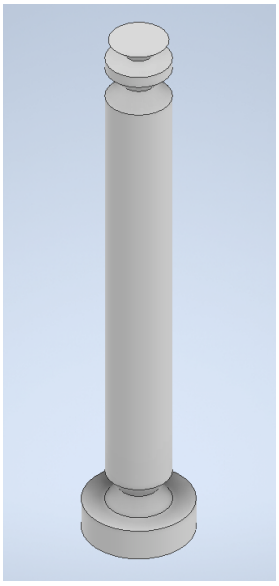

(a) CAD of the pin

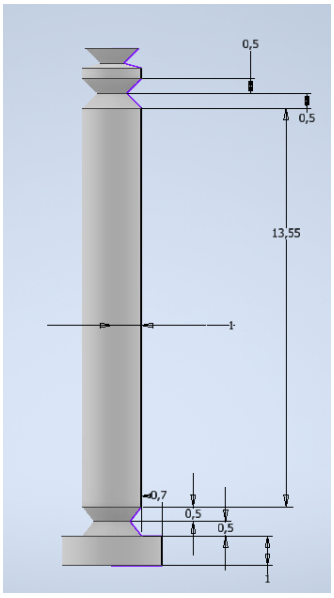

(b) Measurement of the pin

In total, four wires of SMA were used, arranged symmetrically to control the bending of the dorsal and ventral halves of the fin and to reproduce a much more natural movement, respect to the previous case, where the SMA wires were only two. The first experiment about this project was made by a PhD student (William), in which the fin prototype was equipped with two SMA wires arranged in an M-shaped configuration, to reproduce the movement of the fish using the minimal number of actuators. However, the movement and maneuvers of the fin produced were not realistic and so another direction was taken, utilizing four SMA wires. The design was revised to include the additional two independent pairs of SMA wires. With this system, the deformation became more balanced and distributed, increasing the controllability of the movement. In addition, larger deflections, greater stability and higher precision were obtained.

Each SMA wire was crimped to its corresponding conductor and secured with heat-shrink tubing to ensure mechanical stability and electrical insulation.

After the correct positioning of pins and tensioning SMA wires, the next phase was the casting process, in which the silicone was poured into the mold, ensuring complete filling of the cavity and uniform coverage of all embedded elements, guaranteeing completely the embedding of the wires. Once the electrical current was cut off, the silicone's elastic properties guaranteed a smooth transition back to the neutral position.

After pouring, the mold was left for approximately 24 hours at room temperature to allow full curing and polymerization of the material. After curing, the fin was carefully removed from the mold, and the base of the pins broke. Where imperfections were evident, an additional thin layer of silicone was added and allowed to cure for the same time. The same process was repeated a second time for the other half of the fin and then, after that both of halves were ready, they were glued with the use of a thin layer of silicone. At the end of another 24 hours, the complete caudal fin was ready and usable for experiments.

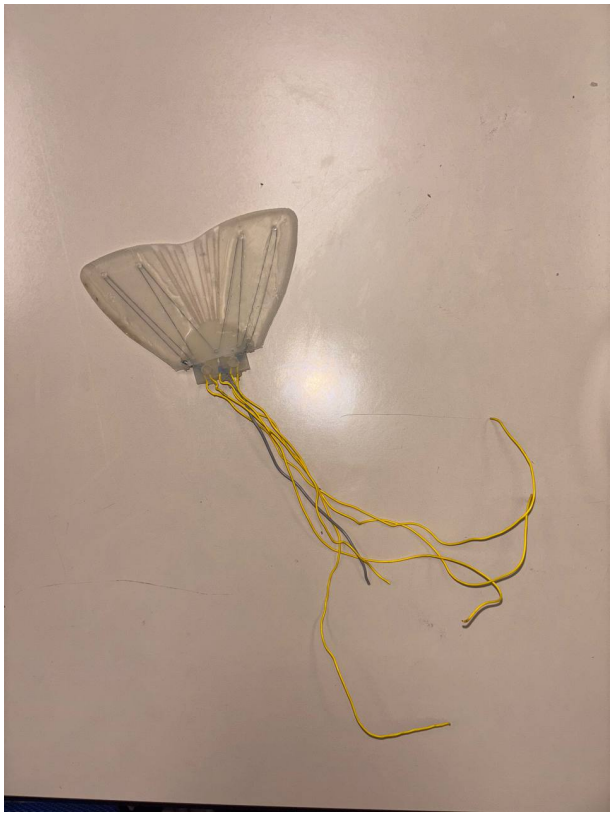

Figure 2.3: Previous Caudal Fin with two SMA wires with M-shaped

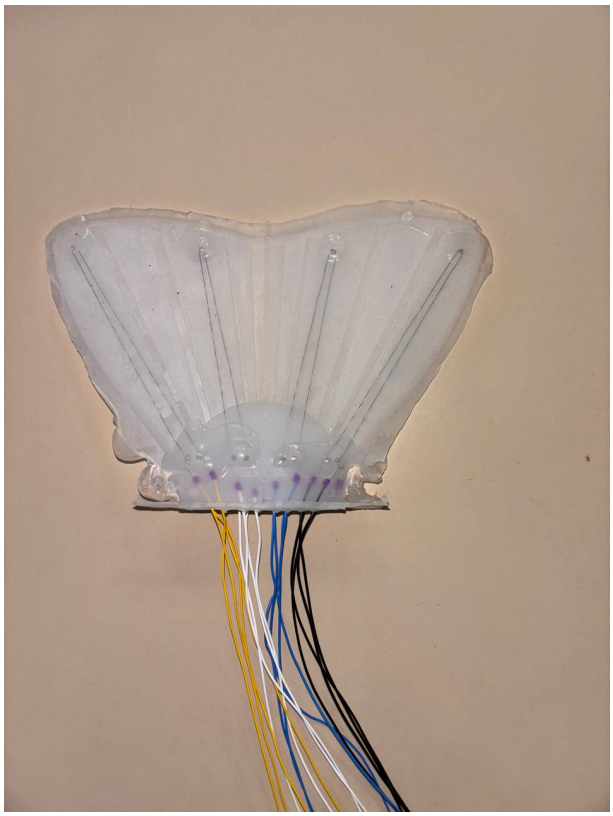

Figure 2.4: Final Caudal Fin with four SMA wires

2.4 Fin Geometry and Deformation Analysis

The design of the caudal fin was based on a particular geometry associated to the fish with carangiform characteristics, in which the thrust generation and the movement are concentrated in the posterior part of the body. This configuration allows to achieve a controllable deformation, focused on the end part of the fin, reducing mechanical and thermal solicitations on the base part.

From a geometrical point of view, the fin features a fan-shaped structure with radial channels extending from the basal bulb toward the free edge. The thickness gradually decreases from 3 mm at the base to about 1 mm at the tip, promoting wider bending and a smoother and uniform curvature.

During preliminary tests, by administering voltage, with the help of the power supply, to the SMA wires, a significant and regular curvature was recorded, with an angle between 15 and 25 degrees, depending on how much voltage was applied. The elastic response of the silicone allow a rapid return to its original position after every cycle of actuation, ensuring a stable deformation over the time.

Therefore, the flexibility and the symmetry of the whole structure allow to obtain a behavior similar to the natural movement of fins of fishes, with a wave propagation that begins from the base to end in the extremity of the fin.

2.5 Assembly Challenges and Improvements

A crucial part of this preliminary phase, to guarantee the success of the next phase, the experimental one, is the correct calibration of the materials, because many problems and difficulties emerged.

The first is related to the correct positioning of the SMA wires in the mold, because with the pouring of silicone the alignment of them can be compromised. Hence the use of resin pins, printed in the same 3D printer, was essential in this positioning part of the wires, and after that, making sure of sufficient tension of them, they were glued with the pins to ensure the right locking even after pouring the silicone.

Another difficulty was the presence of air bubbles during the silicone pouring, which compromised the continuity and the transparency of the material. The solution adopted was to pour slowly the silicone, letting out as much air as possible.

Also the electrical connection required a particular attention, since the contact between the SMA wires and the electrical wires tended to become weaker each time. With the use of crimp between these wires helped to improved the connection and the stability.

Chapter 3

Electronics and Control System

3.1 Electronic system

In the previous chapter, the explanation of the mechanic part of the fin was the main focus, but to make it function, the description and the integration of the electronic part are also important, since it feeds and controls the SMA wires in a precise way, it acquires data of the inertial sensor (IMU) and it exchanges information with an external computer for monitoring and calibration.

In contrast to a traditional rotative actuator, SMA presents a thermal-electric non-linear behavior: a small variation of current can produce a considerable variation in temperature and, intrinsically, in contraction. For this reason, the electronic part can be reduced to a simple "switch", but in a system with various levels:

- generation of an analog command signal (DAC/PWM)
- measurements of the provided current and feedback
- protecting the SMA wires in overcurrent situations
- exchanging data with an external unit (ESP32-S3) for the calibration
- control multiple fins or sections of the same fin

The electronic system designed by Antoine refers to a previous project conducted by William (Phd) and it has been improved since it presented some problems, which will be described and analyzed during this chapter, adding the relative and more effective solution. In Table 3.1, the functional structure is presented and it is equal in both versions of the electronic: the main difference between the old version and the new version is how the currents are measured, which pins of the ESP32 are used and how much the start and the scalability are reliable.

Table 3.1: Functional structure of the electronic control system

Functional Block	Description and main function
Control Unit	Based on a ESP32-S3 microcontroller. Executes the main firmware, generates actuation commands, acquires analog measurements from the SMA channels, and manage a wireless communication.
Command Generation	It converts digital setpoints in analog tensions through a DAC or in a PWM signals. Provides the power driver with the desired current reference for each SMA channel.
Power Stage	Includes the switching MOSFETs and the current-sensing resistors (R_5) for each channel. It provides a controlled current to the SMA wires and it integrates thermal protection and power-limiting circuits.
Sensing Section	It acquires the voltage drop across R5 to estimate the real current on the SMA wire, according to the relation $I_{SMA} = V_{shunt}/R_5$. The signals are sampled by the ESP32-S3 ADC and they are transmitted to the firmware for monitoring.
Inertial Sensors (IMU)	It measure the pitch and roll angles of the robot body. These data are used to analyze the correlation between caudal fin actuation and posture variations.
Communication Layer	Manages data exchange between the microcontroller and the PC, or among multiple boards. Implements Wi-Fi communication

This chapter introduces a descriptive panoramic on Harware Control, Software Architecture implemented on the microcontroller, user interface used during tests and the performed preliminary tests to validate the functioning of the entire system.

3.2 First PCB Version

3.2.1 Objective of the First PCB

The first board was designed as a unit of actuation with four channels, where each channel piloted only a SMA wire and at the same time providing a value of the current to the MCU.

The board also was in charge of:

- communicating with the PC or a "master" board through Wi-Fi/ESP-NOW
- being duplicated to communicate with more fins or more areas of the same fin
- allowing rapid tests

It mus be highlighted that this first version was already functional, but it had some practical limitations that must have been improved.

3.2.2 Structure of the actuation channel

Each channel of the first PCB was structured in this way:

- a MOSFET/power MOSFET attached to the SMA wire
- a current sense resistor in series (R_5)
- an analog line directed to the ADC of the ESP32-S3 board to monitor the drop voltage on R_5
- in some test, a current sense amplifier, to amplify the dynamic measure

The operating principle was a basic one:

$$I_{SMA} = \frac{V_{shunt}}{R_5}$$

where:

- I_{SMA} is the current on the SMA wire
- V_{shunt} is the voltage measured across the sense resistor
- R_5 is the known value of the sense resistor

Better explained, if there is a small known resistance in series with the actuator, each time that a current flows, a small drop voltage is produced. Measuring this drop with a ADC of the microcontroller, it can be obtained how much current goes to the SMA.

3.2.3 First Problem: drop voltage too small

In the first version, to prevent an overheating of the board and to not take too much voltage from the SMA, R_5 was chosen with a low value. Considering the current values used in the experiments (of about 0.5-1.5 A), the voltage across the resistor R_5 was too low to be measured with a good resolution from the ADC of the ESP32-S3.

For example, if $R_5 = 0.05\ \Omega$ and the current is equal to $0.4\ A$, the drop voltage is equal to:

$$V_{shunt} = 0.4 * 0.05 = 0.2\ V = 20\ mV$$

Obviously, this drop voltage is very small and the measure could be damaged and become less reliable with just a little noise, or a drop on the cables, or maybe with a

not calibrated ADC. That is the motivation why an amplifier was adopted, even with its limitations, such as making the board more sensible to noises and saturation.

3.2.4 Second Problem: dissipation on the sense resistor

A possible solution to the previous problem could be increasing the value of the resistor R_5, but another problem arises: the resistor begins to overheat. The power on this resistor is described by the formula:

$$P_{R_5} = I_{SMA}^2 * R_5$$

The SMA requires values of currents as $1 - 1.5\ A$ to move and contract the wire. So, if R_5 is too high, the power on the resistor rises with the square of the current and becomes an hot element on the board and this is a huge problem since:

- it overheats the near components
- it alters the measurement because the resistance varies with the temperature
- the reliability decreases

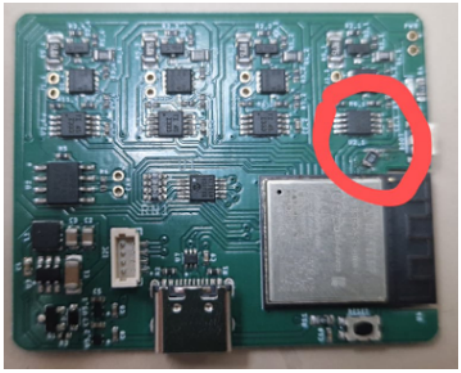

Figure 3.1: First PCB Version

3.2.5 Third Problem: pin assignment and start of the microcontroller

In the first version, some GPIO of the ESP32-S3 were not suitable since some of them were pin of the boot, others were shared with Wi-Fi functions or with ADC channels with an inferior resolution. In some tests, the board did not start in a correct way or it started in a programming mode.

3.3 New PCB Version

As it has already been written, the new version do not change any structural aspect of the system, but it improves the main problems that have already been discussed: varying measurements, non controllable dissipation and a no reliable starting. So, the structure remains the same, but values, pins and some components are chosen in a better way.

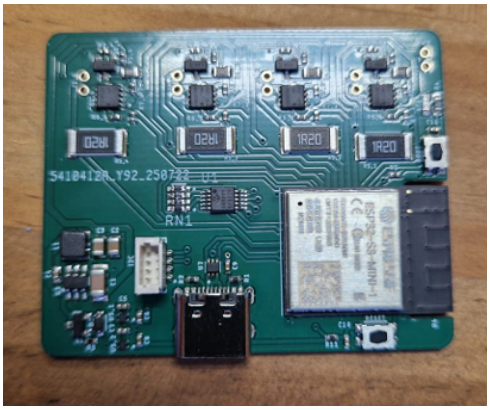

Figure 3.2: New Version of the PCB

3.3.1 New value for the sense resistor R_5

The first modification regards the value of the sense resistor R_5, where the main steps to choose it are:

- choosing the maximum value of the current that has to be provided to the SMA (for example $1 - 1.5\ A$)
- choosing the minimum value of the voltage that has to be read on the ADC (for example $0.1 - 0.15\ V$)
- obtaining the value with the following formula:

$$R_5 = \frac{V_{shunt,min}}{I_{SMA,max}}$$

For example, if a voltage of $0.12\ V$ using $1\ A$ of current is wanted, the value of resistance will be $0.12\ \Omega$, which is a good compromise, because it is enough high to generate a measurable voltage, but not too low to generate excessive power. But in any case, a control on the power has to be done with formulas:

$$P_{R_5} = I^2_{SMA,max} * R_5 = (1\ A)^2 * 0.12\ \Omega = 0.12\ W$$

The value of the power is not too high, so it can be used an higher value for the resistance, fixing it. Another way could be fixing the value of the current, maybe because

the tests need a certain value of it, for example 1.5 A using the same value of the sense resistor, and so the power would be:

$$P_{R_5} = I^2_{SMA,max} * R_5 = (1.5\ A)^2 * 0.12\ \Omega = 0.27\ W$$

Also in this case, the value of the power is not too high, but focusing on the current, to avoid of overheating too much the board, this value is adopted only in the case of short pulses, meaning a small duty-cycle.

3.3.2 Simplification of the measurements

With a voltage drop of about $100 - 150\ mV$, the ESP32-S3 ADC (even without amplifier) is capable of measuring the signal with a resolution good enough for the purpose of the work, because it focuses on driving an SMA, not controlling a brushless motor at 20 KHz. So, in the new version, the current amplifier can be removed or substituted with a more linear one with a minor gain. It is relevant in general because in a system implemented with fewer analog components there are less problems to resolve and, in this case, a better measurement of how much the SMA is overheating. Reducing the steps of the process makes the measure more repeatable.

3.3.3 Pins reassignment and multi-board

In the new version, the allocation of GPIO pins is rearranged, especially the ones for analog acquisition and control of the DAC, because in the first version some of them were involved in the ESP32-S3 boot sequence. This modification made it possible to achieve deterministic startup behavior in all tests and to enable Wi-Fi/ESP-NOW communication without any problem.

After the introduction of the whole hardware of the system, the new version of the electronic was tested with multiple boards arranged in parallel. They communicate via wireless with a maximum of four PCB, where one is the master and the others are the slaves, which report all the measured currents, and then the master put them together and it sends all to the PC. It is important to say that the board was not changed, the only modification that was made was on the network architecture.

The Figure 3.3 shows how the electronic was assembled to be compatible with the whole system.

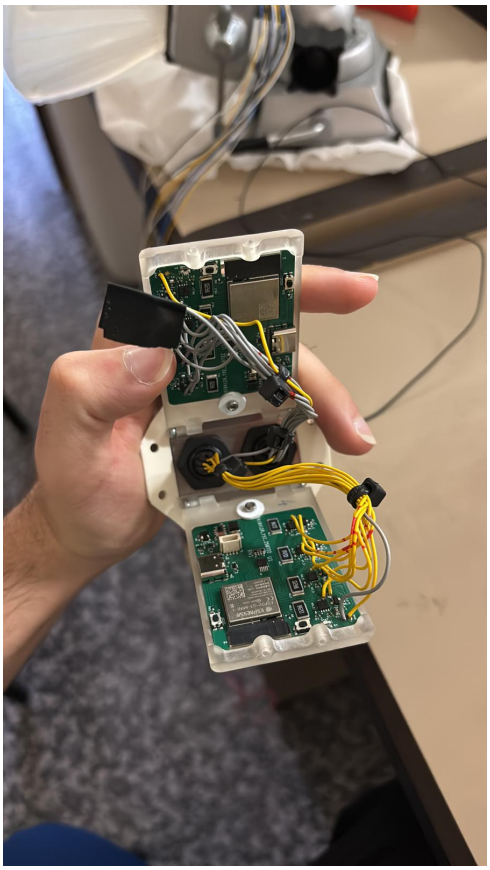

Figure 3.3: Electronic inside the case

A case was constructed, modeled in CAD and printed with the same 3D printer used for the mold of the fin, to allow the integration of the electronic inside the body of the fish. It was designed to fit in the central part of the robot, guaranteeing a compact disposition of the components and an appropriate way to let out the connection for the fin.

The most important part in designing the case was the waterproofing of it, since it is an experimental study and the water could leak in any moment during the underwater tests. Indeed, the enclosure is composed of a silicone seal running along the entire perimeter of the cover and by stainless steel screws that ensure uniform tightening. The design of the case offers mechanical shielding, reducing vibrations transmitted to the board and preserving the integrity of electrical connections.

In this way, the electronic is completely isolated and perfectly integrated with the body of the robot, allowing repeated tests both in air and in water, always making sure that there are not leaks of water since it is always an experimental study and the connection between the fin and the body was not properly closed in an efficient way.

3.4 Software Implementation

In Table 3.2, it is presented with the modules of the firmware.

Table 3.2: Organization of the modules of the firmware

Modules	Description and main function
Communication	It receives the setpoints and it sends the data.
SMA actuation	Starting by a number set between 0 and 4095, it convents this setpoints into analog voltages or PWM signals, it drives the power MOSFETs for each SMA channel, and it the heating phase of the wires.
Acquisition	Periodically, it reads the voltage drop on the resistor R_5 and the IMU data.
Security	It compares the measured current with a maximum threshold, and if necessary, the channel is turned off.
Logging	It organizes the measured data into structured CSV format and it transmits them to the PC for visualization and offline analysis.

Moreover, the generated command by the microcontroller is expressed as a DAC value and the equivalent formula is the following one:

$$V_{cmd} = \frac{N_{DAC}}{N_{max}} * V_{ref}$$

where:

- N_{DAC} is the written value
- N_{max} is the maximum value, in this case 4095
- V_{ref} is the DAC reference value

This formula is crucial to relate the software and the hardware. For example, if in the DAC is inserted the value 2048 and the DAC reference value is 3.3 V, the result is about the half of the DAC reference value, so half of the power, and then it can also be introduced the measured current in all of it.

3.4.1 Protections and safety measures

Since the SMA does not have to be active for a long period of time, some precautions are adopted in the firmware, such as:

- a current limitation
- a maximum actuation time (thermal duty-cycle)
- a condition when the ADC detects a 0 value or a value out of the range

Even if only one of them is broken, the channel is immediately disabled and an error message is sent to the PC.

3.5 User Interface

Since it is an underwater application, obviously there has to be a PC interface, where the user inserts the inputs to pilot the SMA on the fin. This interface allows to:

- send commands to the SMA channels
- show in real time the measured currents
- visualize the state of the IMU (roll, pitch and yaw)

The use of this interface, with the electronic system, was significant in the experimental sessions to activate the SMA wires, record the sensor data and evaluate the deformation of the caudal fin. The experiments were based on a standard procedure, that follows these steps:

- System initialization, where the system is activated and the board is powered on, performing an internal self-check and the communication is verified with all active channels. If any module fails to respond, the system enters a safe idle state and notifies the user through the serial console.
- Wireless connection setup, where the user connects the board via Wi-Fi.
- Interface configuration, where the user sets the test parameters, such as the number of SMA channels to activate
- Actuation phase, where the board generates the corresponding DAC/PWM signals for each channel.
- Data acquisition, where the data (such as timestamp, DAC command per channel, IMU orientation and voltage and current readings) are stored in a CSV file.
- End of test and Data validation, where, at the end of the activation cycle, the system returns at the beginning state and the collected data are post-processed to correlate current, deformation and fin orientation.

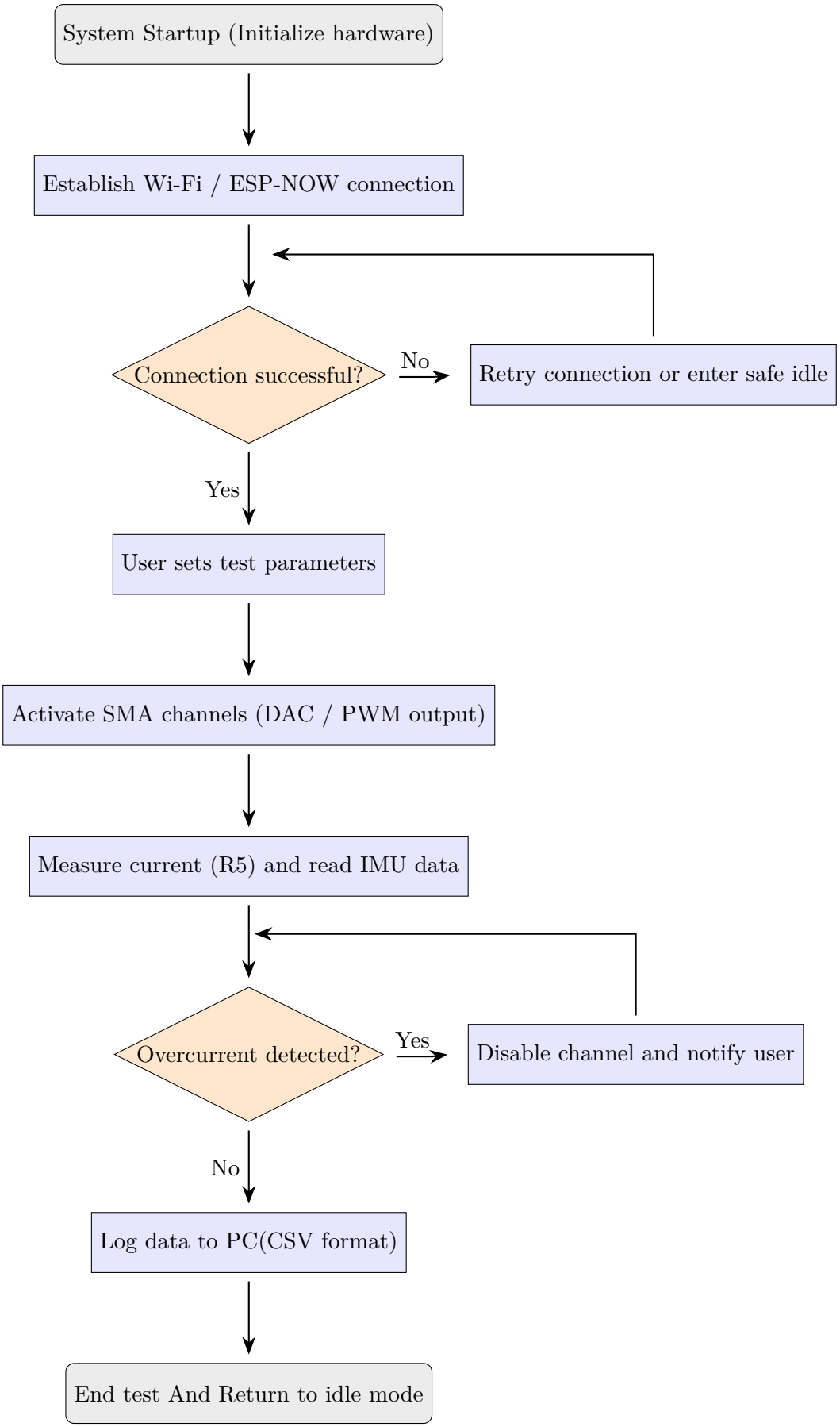

Figure 3.4: Flowchart of the control and data acquisition logic implemented on the ESP32-S3.

3.6 Preliminary Tests

Preliminary tests were made to understand if the board measured all the parameters in a good way and if the current does not overheat the board or near components.

3.6.1 Test on a single channel

In this first test, only a channel was activated with only one SMA wire, with a given command of 50% of the DAC and it was shown:

- the contraction of the fin
- the measured current on the ADC
- the absence of reset

The test was repeated for all four channels to verify that the cabling of the fin was correct.

3.6.2 Test on multiple channels/multi-board

Consequently, the validation of more channels simultaneously was essential for the purpose of the work, and, moreover, the functioning of more PCB in parallel through ESP/NOW. The master sent some commands and the slaves responded with the measurements. This confirmed the utilization of it for a robotic fish with more actuators.

3.6.3 IMU Validation

Lastly, with the activated fin, the measurements with the IMU orientation were recorded to verify the variation of roll and pitch angles of the body through the movement of the fin, and the vibrations were not a problem for the sensor.

Chapter 4

Sensors and Measurement Setup

In the previous chapter, the main objective was the explanation of the modeling of the electronic and the control system, where a measuring component was necessary to add, to provide the main information of the rigid body of the robot during operation. The integration of an inertial sensor (IMU) inside the electronic system is the key to understand better the dynamic behavior of the robot, particularly to analyze the imbalance generated by the actuation of the caudal fin.

The focus of this chapter is to describe the entire process of the integration of the IMU, from the mechanical assembly and the electronic connections, to the management of the software and data acquisition. Moreover, various aspects of it would be presented in the chapter, such as:

- the calibration methods, of filtering and synchronization with actuation commands
- experimental methodology, adopted for the system validation and for the study of the dynamic response of the robot during the activation of the SMA

The aim is to demonstrate how the given information of the IMU can be used to correlate the current, provided by the actuators, with the variation of the inclination of the body, and so with the actuation and the resulting imbalance of the caudal fin.

4.1 Hardware IMU Integration

The IMU adopted in this system is a sensor with six degrees of freedom (DoF), equipped with an accelerometer and a gyroscope, both with three axis. It is integrated directly on the electronic board, principally to reduce the length of the various connections and to minimize the electronic noise caused by the signal. The sensor communicates directly with the microcontroller ESP32-S3 through an interface I^2C, able to read the data in real-time with a value of frequency between $100 - 200\ Hz$.

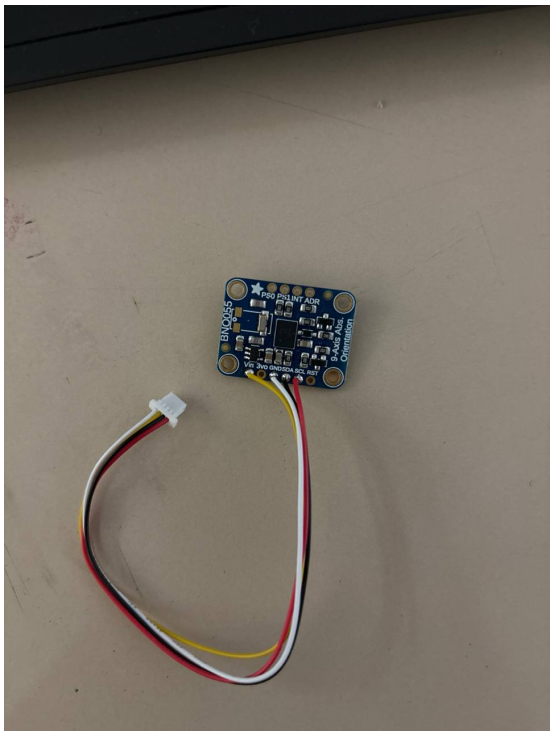

Figure 4.1: IMU Adafruit BNO055 used for the study

The inertial sensor adopted in the study for the realization of the measuring system is the BNO055, assembled on an interface board Adafruit. It is an IMU sensor with nine degrees of freedom, which integrates a tri-axial accelerometer, a tri-axial gyroscope, a tri-axial magnetometer and an embedded microprocessor dedicated to sensor fusion.

In contrast to traditional IMU sensors, which provide only the raw values of the three sensor, the BNO055 implements an internal sensor fusion algorithm (based on an Extended Kalman Filter), which is able to provide directly the Euler angle or the corresponding quaternions, simplifying the elaboration of the microcontroller.

This sensor was adopted mainly for two reasons:

- the possibility to obtain roll and pitch angle estimates, already compensated by the gyroscope, reducing the complexity of the filter already implemented in the ESP32-S3 board
- the simplicity of the integration through I^2C interface

The sensor works with a voltage alimentation of $3,3\ V$ and it was connected directly on the control board, which manages the periodical reading of the data and the following transmission on the PC for the analysis.

During the assembly phase, the necessity was to define precisely the position of the sensor on the rigid body of the robot and its orientation with respect to the axis. The sensor was fixed in a central area of the structure, proximately to the center of gravity of the body, in order to reduce the effect of the linear accelerations of the mechanical

oscillations and to obtain a more representative measurement of the overall rotational motion.

The IMU orientation with respect to the body was defined to align the x-axis with the longitudinal direction of the body and the z-axis with the vertical one, mainly to simplify the interpretation of the data and to understand directly the pitch movement from the acceleration contribution along the principal axis.

4.2 Data Acquisition

To better analyze the data provided by the IMU, a fixed reference system was defined and positioned on the body, denominated *body frame*,which is useful for measuring all the accelerations and angular velocities. This system is aligned with the principal geometric axis of the body, while the global reference system (*world frame*) has a vertical component that coincides with the direction of gravity. During the functioning, the microcontroller reads the raw values of acceleration and angular velocity, it normalizes them, and it converts them using scaling factors provided by the manufacturer of the sensor. The data are sent to the PC via Wi-Fi and they are recorded in a CSV file with the values of current and voltage provided by the actuation channels.

The structure of the file for each time instant includes the acquisition of numerous data, such as:

- time
- acceleration in the three axis
- angular velocities
- actuation command (expressed with DAC/PWM values)
- current for each SMA wire
- pitch, roll and yaw angles

This organization of the data is helpful to conduct synchronized analysis with the electrical parameters and the dynamic response of the system.

4.3 Experimental methodology

The system was used to study the effect of the actuation of the caudal fin on the structure of the robot. Tests were conducted both in air, to isolate the inertial effects, and in water, to evaluate the influence of the hydrodynamic forces.

During these tests, the fin was activated in various modes, such as:

- actuation of each SMA wire
- actuation of couple of SMA wires (inferior half and superior half)
- actuation in the opposite phase (making an S-form movement with the fin)

In air, the objective was to observe how the distribution of the forces of the fin influenced the imbalance of the rigid body and the variation of the pitch angle. The actuation currents were limited within certain values, and at the end of each actuation cycle, a cooling period of time was adopted to avoid overheating of the material.

In water, the mechanical configuration and the actuation protocol remained constants. The behavior of the system was more stable, but with a reduction in angular width, caused by the hydrodynamic resistance. Even in underwater condition, the IMU sensor tracked the pitch angle in real time, showing how the actuation of the caudal fin generates a little and measurable rotational torque.

The data were collected and analyzed later in terms of angular width, pitching, response time and stability of the signal. The correlation between the average current that was applied on the SMA and the pitch variation confirmed the existence of a direct relation between the intensity of the actuation and the imbalance. This result is important to better understand the role of the caudal fin in a robotic fish and to develop a feedback control strategy, where the IMU sensor could be used as a feedback sensor to maintain the dynamic equilibrium of the robot.

Chapter 5

Static Calibration

The main objective of this chapter is to perform experimental tests and to accurately characterize the behavior of the biomimetic caudal fin, actuated through SMA wires, evaluating how electrical control quantities influence the static deformation of the fin. For this first experiment, tests were performed with the fin attached to a grip, to isolate the effect of the actuator as much as possible, excluding also movements of the body since it is exclusively to see how the fin moves. Later, the body of the fish will be used to calculate the stabilization of the fish, but for now the objective is to see the relation between the deflection angle and the resistance, and if this is a linear relation, despite the non-linearity of the SMA.

5.1 Test bench and Instrumentation

Calibration tests were performed by fixing the fin to a grip, mainly to ensure a rigid and play-free mechanical constraint, allowing to completely eliminate oscillations of the body of the robot, isolating and concentrating only on the deformation of the fin.

The grip was positioned at the base of the fin, and then the whole structure was dipped in a tank full of water, and during the experiment it remained that way. The water is important in this experiment not only to test the fin in a real condition, since it is used in the application of robotic fishes, but also because it influences the cooling of the SMA and the hydrodynamic resistance, opposed to the movement of the fin.

The electronic was used to send the right commands to the fin to allow the movement of a pair of SMA wires, sufficient to acquire electrical data. The board was charged from an external power supply, and communication with the PC was made through a serial port. On the PC, data were recorded in real-time, saving them in columns: time, DAC value, $V1$ tension, $V3$ tension, and SMA resistance.

To measure the deflection angle of the fin, the software Tracker (video analysis and modeling tool) was used. A camera was positioned, orthogonally to the fin; visibility was optimized applying a fixed reference on the tip of the fin.

5.1.1 Test Protocols

The tests were divided into two main phases, the first related to the electrical test and data collection, and the second for measuring the angle in the videos, through the software Tracker.

The first phase, for each DAC value (3000, 3200, 3400, 3600, 3800), ten unrelated (one to the other) tests were executed. The DAC values were chosen sufficiently high to activate increasely the fin, since they are approximately near the maximum value of 4095. Each test consists on activating the SMA, maintaining constant the DAC value until the stationary condition is achieved. During the test, some values were recorded such as, time, $V1$ tension, $V3$ tension and SMA resistance. Each test started with the same thermal condition for the fin: before proceeding with the next test, there was a certain time, cooling time, to let it cool completely. This part was crucial to avoid that the residual temperature influenced the initial resistance of the next test and the time to reach the regime.

After the electrical data collection, for each DAC value, a video was recorded. The fin was actuated, and when it was arrived at the stationary position, the deflection angle was measured with Tracker. For the same DAC value, a set of ten tests were performed to have a range value of data, to see the repeatability and to avoid eventual errors caused by slight residual oscillations.

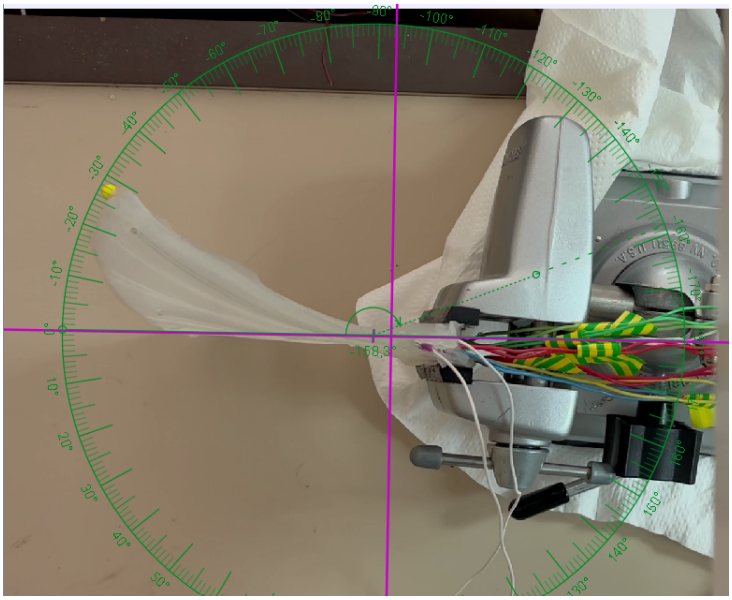

Figure 5.1: Deflection angle measured through Tracker

5.1.2 Data Acquisition and Processing

The firmware on the microcontroller collected real-time data in a file structured in the following way:

- tempo_ms: timestamp in milliseconds
- DAC: value sent on the actuator
- $V1$: tension on the SMA
- $V3$: tension on the shunt resistance
- R: resistance of the SMA, measured through tension and shunt resistance

Each test generated a sequence of samples at high frequency. The resistance curves showed the usual transient-plateau behavior: SMA heating caused the resistance to drop quickly upon activation before steadily stabilizing toward an asymptotic value. The quantity of interest for the calibration was this steady-state value.

For each test, the last twenty values of the resistance were selected because they corresponded to the stationary region of the curve. The mean of these samples was computed, yielding a stable resistance value for that specific trial. Repeating the operation for the ten tests associated to the same DAC value, it was possible to obtain the final mean and standard deviation of the steady-state resistance. In the figure below, the resistance curve over time for a DAC value equal to 3000 is showed and it is possible to see that at the beginning the values of resistance are high and then, after a certain amount of time, the values decrease because of a more contraction of the fin, until a plateau-transient region is reached (marked in red in Figure 5.2).

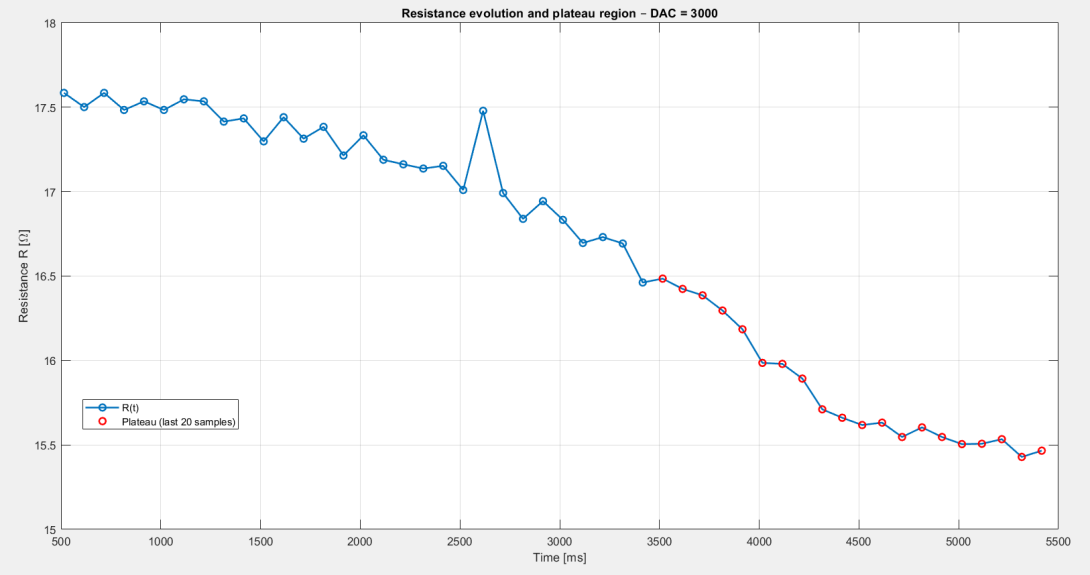

Figure 5.2: Resistance evolution and plateau region – DAC = 3000

The same procedure was applied to measure the deflection angle: for each DAC value, ten measurement were made and then, from these, the mean, standard deviation and coefficient of variation were calculated.

5.1.3 Uncertainty and Repeatability

This is an important part to take in consideration when SMA actuators are used. The main sources of uncertainty identified in this study are:

- Residual Temperature in the SMA wire at the beginning of each trial, which could influence the heating velocity and the final value of the resistance.
- Non-Uniform thermal dissipation during actuation, due to the interaction with water and fluctuations in ambient temperature
- Measurement Noise introduced on the control board, particularly in the voltage sensing stages
- Errors in the angle measurement performed through Tracker, resulting from tiny residual oscillations that have not been completely removed or from manual maker selection

The standard deviation of the resistance and angle readings throughout the ten trials for each DAC command was used to evaluate the repeatability of the measurements. The resistance values indicated a greater dispersion, which is consistent with the considerable temperature sensitivity of SMA materials, but the angle measurements demonstrated good consistency.

This initial research emphasizes how crucial it is to take boundary conditions and thermal impacts into consideration when utilizing SMA electrical resistance as a possible fin deflection indication. The ensuing sections will look at these aspects in more detail.

5.2 Relation between Current, Resistance and Deflection Angle

A crucial part related to the SMA as an actuator was the comprehension of the relation between the current, which flows on the wire, and the variation of the electrical resistance and the static deformation of the caudal fin. This relation was not so obvious and it had to be obtained experimentally, due to the soft system of the fin and the strong dependence on the thermal condition.

5.2.1 Electrical characterization of the SMA (current–resistance)

The SMA wire behaves like a resistor with a positive temperature coefficient: when in the wire flows current, the power dissipation $P = I^2 * R$ causes a rise up of internal temperature, which inducts a mechanical contraction and a reduction of electrical resistance.

This reduction is visible in the experimental tests, since the initial phase is characterized by a rapid descent of resistance, followed by a gradual approach to a stationary value.

The imposed DAC value controls the entering current to the actuator (through a driving circuit and a shunt resistance). Therefore, each level of DAC corresponds to a different level of heating the SMA and contraction of the wire.

During each trial, the instant resistance of the wire was monitored (through the tension $V1$ and $V3$ provided by the board). The trend of the resistance tends to a state of thermal balance, that represents the perfect condition to correlate the electrical and the mechanical quantities.

5.2.2 Static calibration: resistance vs. deflection angle

The following approach was adopted to obtain the static model that connects directly the electrical resistance of the actuator to the deflection angle of the fin:

- for each DAC value, ten trials were performed
- for each trial, the last twenty samples of the resistance were selected, because they correspond to the regime area
- it was calculated the mean of these samples, obtaining the value of the stable resistance of the trial
- the mean of the ten trials provided the mean value of the resistance for that DAC value
- a similar operation was performed for the deflection angle, obtained through Tracker

Table 5.1: Mean resistance, deflection angle and steady-state SMA resistance for each DAC level

DAC	$\theta_{\mathbf{mean}}$ **[deg]**	$R_{\mathbf{mean}}$ [Ω]	$R_{\mathbf{std}}$ [Ω]
3000	19.57	15.4215	0.3504
3200	21.29	15.3754	0.2082
3400	25.30	15.4199	0.3425
3600	28.05	15.1337	0.1210
3800	30.03	15.2939	0.0949

In Table 5.1, there are the static calibration results obtained for the five DAC levels considered. For each of them, there are the mean deflection angle measured through Tracker, the mean steady-state resistance of the SMA, and the corresponding standard deviation computed over the ten trials performed.

As the data suggested, there is a good repeatability in the angle measurements and a larger variability in the resistance values.

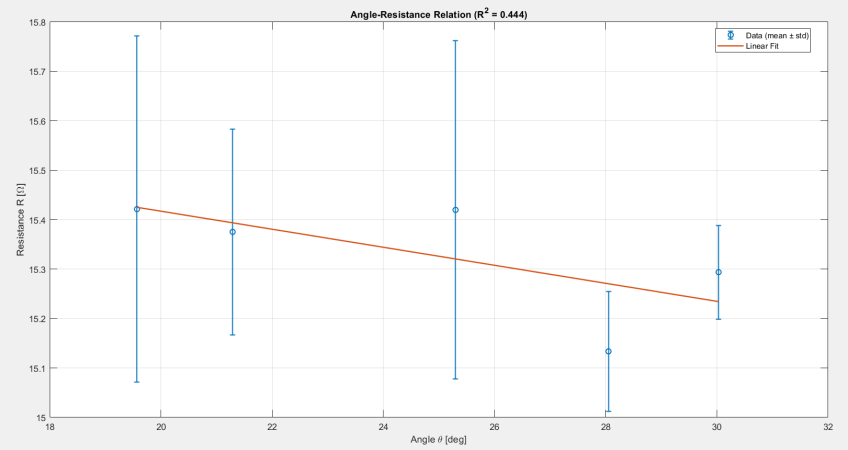

Figure 5.3: Angle-Resistance Relation and Linear Fit

Table 5.2: Raw deflection angle measurements for each DAC value

Trial	**3000**	**3200**	**3400**	**3600**	**3800**
1	18.0°	19.7°	25.1°	27.9°	29.8°
2	18.4°	20.1°	24.8°	28.3°	30.0°
3	19.0°	20.0°	25.7°	28.5°	30.2°
4	19.1°	19.2°	25.5°	28.1°	29.9°
5	18.5°	19.5°	26.0°	27.8°	29.5°
6	21.0°	22.2°	25.6°	28.0°	30.5°
7	20.8°	23.0°	25.0°	27.7°	30.1°
8	20.1°	23.5°	24.9°	28.3°	29.8°
9	20.3°	23.1°	24.5°	28.2°	30.4°
10	20.5°	22.6°	25.9°	27.7°	30.1°

Through this process, for each DAC value an angle and a resistance were associated to analyze the relation between the deflection angle and the resistance of the SMA.

From the experimental tests, an inversely relation was obtained: increasing the deformation of the fin (consequently the angle), by feeding current on this, the electrical resistance of the SMA decreases.

5.2.3 Inverse model: angle estimation from resistance

Once all values were obtained, a linear regression was made by following this formula:

$$R = m * \theta \ + \ b$$

where m is the angular coefficient (expected to be negative) and b is the intercept, so the value of the resistance when the deflection angle is equal to zero.

With the inverse model, it is possible to obtain the angle, more useful for the control application:

$$\theta = \frac{R - b}{m}$$

Theoretically, this model could estimate the deflection angle, knowing only the electrical resistance. However, as it is discussed in the following chapter, the experimental variability observed in the tests makes this estimate affected by a significant uncertainty.

5.3 Preliminary PID controller design

This section presents a first approach of designing a PID controller for this particular application, keeping in mind that the objective is not to obtain the final model of the controller, but to define a first approximation of a simplified linear model, improving the dynamic behavior of the closed-loop system.

It is important to remind that the proposed model is not the final one and it does not faithfully describe the real behavior of the fin underwater, but it is a point to start the analysis of the PID controller in this application.

5.3.1 Initial Model

As already explained in previous sections, the static characteristic of the SMA wire leads to a linear relation between the electrical resistance and the deflection angle of the fin. From this relation, the conclusion was that the coefficient R^2 was really low (≈ 0.44), which highlights a data dispersion and a dependence on thermal conditions.

Despite these limits, a simplified dynamic model of the system was implemented, represented by the following first order transfer function:

$$G(s) = \frac{2.304s \ + \ 11.85}{s \ + \ 5.562}$$

The objective of implementing a controller is:

- improving the velocity of response of the system
- having acceptable overshoot values
- guaranteeing a stable behavior in closed-loop

Initially, it was simulated a step-response for the system, without the controller.

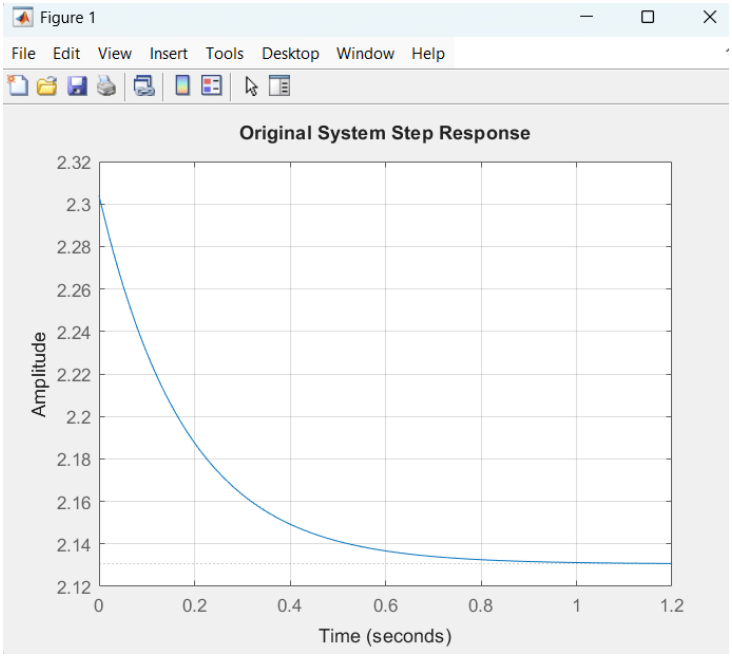

Figure 5.4: Step-response of the system with no controller applied

As the Figure 5.4 shows, the system is stable, but not so reactive.

5.3.2 Procedure with MATLAB

The controller was completely designed with MatLab, following a modified version of the Ziegler-Nichols method for the step-response.

To enter more in details of this method, the procedure applied was the following:

- generating the step-response of the model $G(s)$
- estimating two important parameters of the proposed method: L, the dead-time, and T, the time constant. They were estimated starting by two significant points (28.3% and 63.2% of the final value)
- computing the parameters of the PID controller (K_p, K_d, K_i) using the proposed formulas of the Ziegler-Nichols method
- designing of the controller, using this formula:

$$C(s) = K_p * (1 + \frac{1}{T_i * s} + T_d * s)$$

- evaluating the performances of the closed-loop system through the stepinfo function, principally studying the rise time at 95 %, the overshoot and the hold time

After this procedure, the obtained parameters for the model where sufficiently acceptable, considering $K_p \approx 2.0$, $K_i \approx 120.8$, $K_d \approx 0.026$. From these parameters, it is possible

to understand that the controller is really aggressive, focusing more on a rapid response and a prevalence on the integral action. In the Figure 5.5, the used PID controller for simulations is shown.

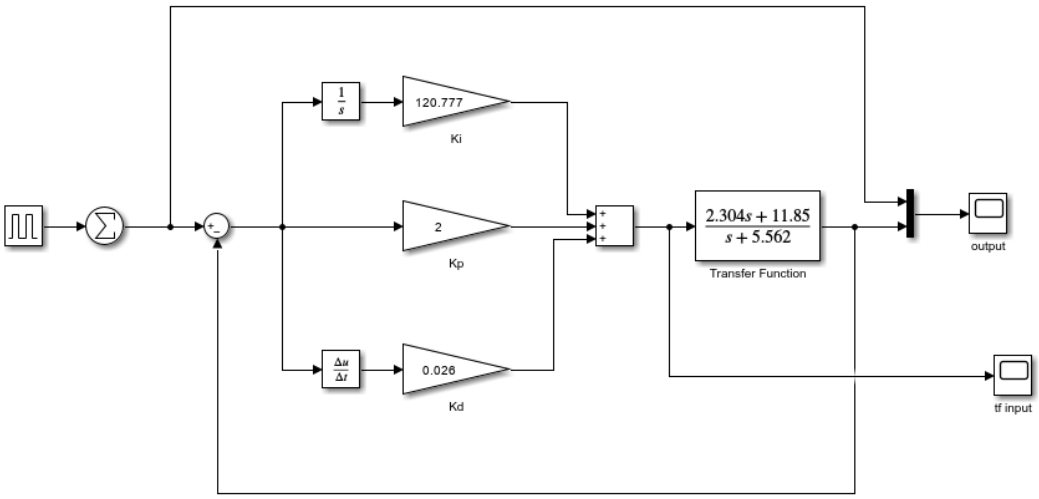

Figure 5.5: PID controller for simulations

5.3.3 Simulation Results

By comparing the model $G(s)$ and the designed PID controller, the difference is really clear. It can be observed that:

- the rise time is practically zero, suggesting that the regime value is rapidly achieved
- the overshoot value is 0.5%
- the steady-state of the system is achieved in $0.05 - 0.1$ s, so more rapid than the original system

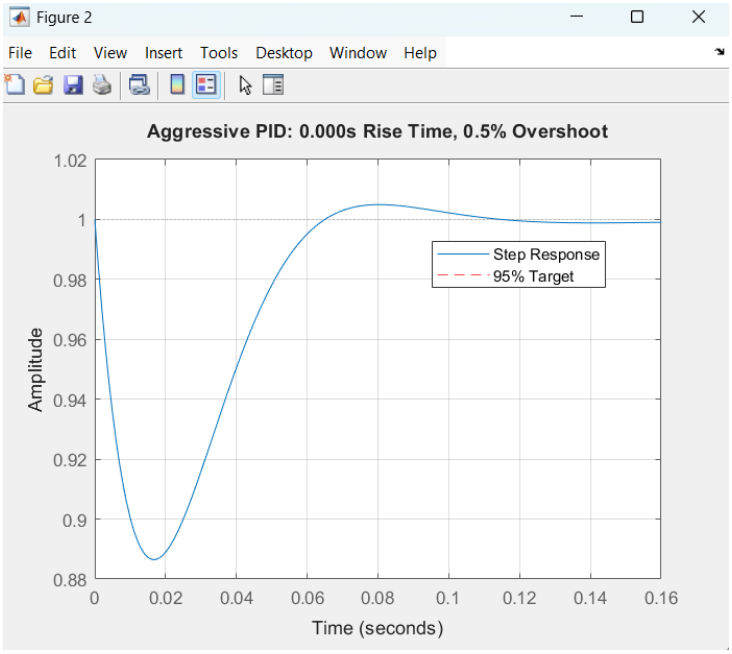

Figure 5.6: Step-response of the system with an aggressive PID controller applied

As the Figure 5.6 shows, the steady-state value is rapidly achieved, with no significant oscillations.

Confronting the two systems, it is possible to see that the original system takes one second to stabilize itself, while the PID system rapidly achieves the final value, remaining close to the reference. In the Figure 5.7, the comparison is shown.

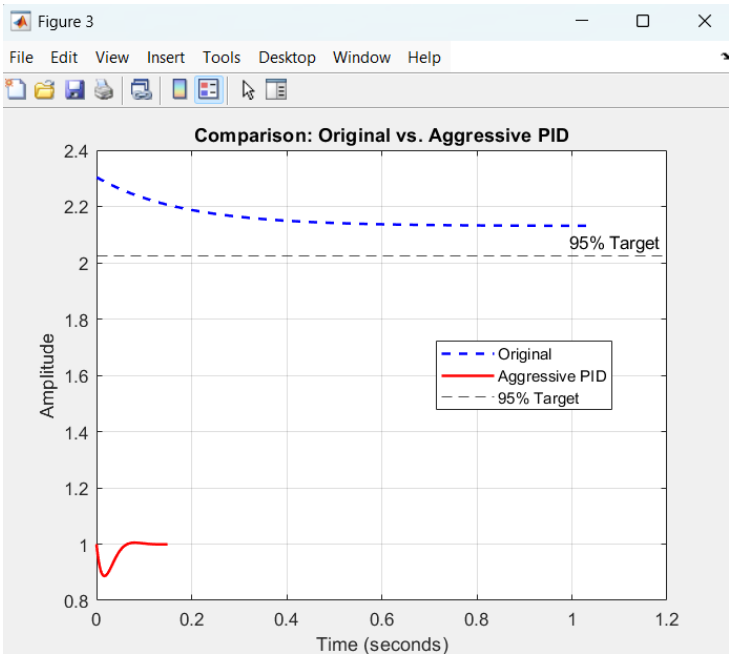

Figure 5.7: Comparison between the two systems: in blue the original one and in red the controlled one

5.4 Results and Discussion

In this section, the results are presented and discussed, obtained by the combined analysis of electrical data and angle measurement. The main focus is to comprehend the quality of the calibration and the reliability of the linear model.

5.4.1 Qualitative analysis of the fin motion

The videos show that the SMA actuator was able to generate coherent and reproducible deformations. Increasing the DAC value, it is visible also a gradual increase of the deformation of the fin, until a limit current is reached, for that particular DAC value.

During the static trials, the fin reaches a stationary configuration, with no oscillations, which is a clear sign that, after the system cooled down between one trial and the next one, there is a predictable behavior for the same actuation level.

5.4.2 Quantitative analysis of calibration results

Elaborating the electrical data, it turned out that the resistance of the SMA presents a non-negligible variability between trials, and this is more pronounced in these data with respect to the measured angles through Tracker.

In the linear model $R = m*\theta + b$, the angular coefficient is negative, as predicted, but the value of the determination coefficient R^2 is very low, precisely 0.4437, which implies that the data sprawl does not allow to accurately explain the linear model. The numerical result of the linear relation is:

$$R = -0.0182 * \theta \ + \ 15.7821$$

The principal causes of this sprawl could be:

- thermal variation between trials
- non-similar cooling times between trials
- SMA sensibility to little ambient variation
- measurement noise in circuits
- slight differences in the fin positioning and in the fluid dynamics of the water during trials

There is a reduction in the linear relation between electrical quantities and deformation for SMA actuators in underwater environment, where there is slow thermalization and dependence on external conditions.

Moreover, the non-negligible variability is explained by the marine environment and the geometry of the fin, that could increase this factor, making the resistance less useful to explain the general trend, despite of the direct measurement of the angle. Therefore, the resistance can be used as qualitative information, for identifying the operation range of the SMA and detecting possible anomalous conditions, such as overheating or insufficient heating.

In conclusion, the linear model represents a first approximation of the system behavior and, in the future works, useful to compare alternative fin designs.

5.4.3 Limitations on the design PID controller

As the results show, the PID controller is able to:

- increase the rapidity of the system response
- guaranteeing an acceptable overshoot
- ensuring stability

But there are some problems that have to be taken in consideration:

- this model is a simplified version of the real behavior of the fin actuated by the SMA
- the static calibration resistance-angle presents a low coefficient R^2, highlighting a data variability and the dependence on operating conditions
- simulations were not performed on the fin, mainly because the model is not sufficiently reliable to simulate the real dynamic behavior underwater
- the real system is characterized by non-linear limitations, such as the thermal hysteresis, cooling effects of the fluid and variable dead-time, which cannot be simulated by a first order transfer function

Therefore, the designed PID controller has to be used as an exploration tool, demonstrating that the system can be stabilized and a rapid control feedback can be achieved, but also a foundation for experiments in future works. Starting from this, there are many things to implement, such as improving the dynamic modeling of the actuator and designing more advanced models that can be adapted to the non-linearity of the application.

Chapter 6

Effects of the Caudal Fin in the Pitching Stabilization

This chapter analyzes accurately the dynamic behavior of the whole system (fin and body of the fish) through the controllable actuation of SMA wires. The objective is to understand how the fin deformation, obtained in various modes for which the SMA is turned on, affects the attached rigid body, particularly in pitch and roll angles.

Remembering that the fin has four SMA wires, two in the superior part and two in the inferior part of the fin, the modes used in this experiment are essentially four:

- actuation of the inferior part, which suggests that the fin tends to flex upwards and to lower the head of the fish body
- actuation of the superior part, where the fin is excepted to flex downwards and to rise forward the body
- simultaneously actuation of all four SMA, which generates a more symmetrical deformation and a more stable pitching
- asymmetric actuation of the two fin halves (inferior and superior), making an S-movement, which generates a more fluid and natural movement, similar to a wave, making the body more stable

All of these are only hypothesis and to validate them, data acquisition and monitoring of the parameters were made for this experiment. It was done to relate the actuation parameters (width, rise and fall times, phase shift) with the actual response of the mechanical system.

The focus of this experiment is to isolate the only behavior of the caudal fin and to see how it affects the whole body, without the presence of the other fins of the fish.

6.1 Experimental setup

6.1.1 Mechanical Structure and Prototype Assembly

A simplified prototype was assembled to conduct the different tests. The body of the fish was simulated by a tube of rigid plastic, with sufficient length and diameter to match the size of the caudal fin, making a good approximation of what will be the future body of the final fish. At one of the two ends of the tube, the caudal fin was fixed, meanwhile in the other end, the electronic system was placed, in order to balance the whole weight and to keep the center of mass as near as possible to the center of the fish.

This arrangement turned out to be optimal because on one side, the fin was able to perform the deformation, and on the other one the electronic system, able to connect the whole system through wires, internally to the body. At top center of the body, the two alimentation wires come out and they are connected to an external power supply, to apply the voltage to make the whole system works.

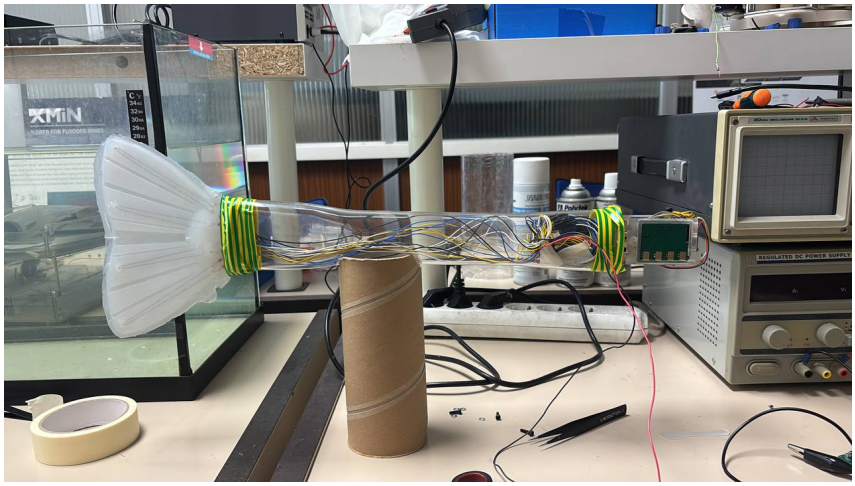

Figure 6.1: Whole setup of the prototype

As the Figure shows, the assembly was done rapidly, but in a functional way, using hot glue and tape, which were able to firmly maintain the components. In the future, there will not be this type of fixing, but a more mechanical one, printing connectors for the fin; but for the moment, it was a rapid solution to apply.

6.1.2 Control Interface

As explained in previous chapters, the electronic system is an ESP32 board, chosen to manage the DAC signals generation and the wireless communication via WiFi.

The control uses trapezoid profiles, divided in three main phases: up, hold and down. Periods and maximum width of these phases could be regulated. The parameter cool

defines the waiting time between a movement of the fin and the next one, useful to avoid thermal storage.

The four modes that can be selected in the firmware are:

- Mode 0: S-movement, where there is a time lag between SMA wires, generating a sinusoidal wave
- Mode 1: all the SMA are activated simultaneously
- Mode 2: only the inferior half of the fin (with two SMA wires) is activated
- Mode 3: only the superior half of the fin (with two SMA wires) is activated

The communication between the board and the PC were made via WiFi, with the UDP protocol and after the test, there is the data acquisition generated, including the IMU measurements, the time and the state information.

6.1.3 Sensors and Data Acquisition

The inertial sensor used, IMU BNO055, is able to provide the orientation angle roll, pitch and yaw, besides angular velocities and linear accelerations. This compact and precise device, which also provides a sensor fusion filtering, returns the Euler angles without external elaborations, that could be complex.

During the trials, the IMU was directly fixed on the body of the prototype, since the electronic system has been fixed on one side of the body as it is already been explained, in a central position and aligned with the longitudinal axis of the body. This position is strategic since it reduces the effect of local oscillations of the fin and to detect the whole movement of the body.

The data are collected in regular intervals ($100 - 150\ ms$) and they are sent to the PC in real time and then processed. Each sequence alerts, and sends to the PC, the beginning and the ending of the trial.

The required parameters are the following:

- Euler Angle: roll, pitch, and yaw (all measured in degrees)
- Angular Velocities: $g_z,\ g_y$ and g_z (all measured in rad/s)
- Linear accelerations: $a_z,\ a_y$ and a_z (all measured in m/s^2)
- Calibration State: the one of the sensor to verify the reliability of the data

All these parameters are useful, not only to evaluate the rotation of the body, but also to identify the dynamic of the movement through velocities and accelerations.

6.2 Experiments and Procedures

6.2.1 Strategy for Experiments

The objective of this experiment is to explore and study all the various modes of actuation of the fin and to evaluate the effect of the parameters on the behavior of the fin and of the body.

Each mode was tested by changing certain parameters, such as:

- DAC width, from 2200 to 3400, to observe the dependence of the power provided
- actuation times (up, hold and down), with values between 150 and 300 ms, to control the velocity of deformation
- cooling time, in a range from 1000 and 2800 ms, to avoid overheating
- phase shift, applied only to the S-mode, with values between 200 and 260 ms

Another parameter that could be chosen is the number of strokes of the fin, but for the experiment it was limited to a maximum of two, to ensure that the thermal and mechanical conditions remained comparable between trials. At the end, for each mode, a matrix of the chosen values was constructed for the ten trials, to see the different combinations of the parameters.

6.2.2 Procedure and Data Collection

Before each trial, a quick check to see if the IMU was correctly calibrated was done, also to verify if all channels were properly connected. After that, at the beginning there were some tests with an external voltage, provided by the power supply, of 5 V to avoid excessive stress, later increasing it until 14 V.

Through the terminal on the PC, all the parameters were inserted, the width, the various times, the number of strokes of the fin and the actuation mode. After that, the command start is sent and then the trial begins. During the actuation, the IMU continuously records the data and it sends them to the PC, where they are saved. After the trial, the ESP32 board waits a certain cooling time, specified when the parameters are inserted, and then it is ready to receive other commands. A total of ten trials were performed for each mode, to verify the repeatability and to identify eventual differences due to the temperature or the residual deformation of the SMA wires.

6.3 Actuation Configurations and Trials

Going into detail, the different actuation modes have different repercussions on the movement of the caudal fin and of the body. The objective for each mode is to evaluate the

dynamic behavior of the rigid body, with a particular attention to the pitching inclination induced by the oscillation of the fin.

6.3.1 Mode 0 - S-movement

This mode is more similar to the natural movement of fishes, where the deflection of the fin is not uniform and it generates a wave along the profile of the fin. This was possible by introducing a phase shift between channels.

In the Table below, the imposed parameters for each trial are reported. The firsts represent soft strokes of the fin (low width and short times), going forward with combinations with more width and longer times, to approach the limit of acceptable performance without overcome thermal constraints.

Table 6.1: Used parameters for each trial in Mode 0 (S-movement)

	amp	up [ms]	hold [ms]	down [ms]	dphase [ms]	cool [ms]
1	2400	150	150	150	260	1000
2	2600	200	200	200	240	1200
3	2800	250	200	250	220	1400
4	3000	300	250	300	220	1600
5	3200	300	300	300	200	2000
6	3000	150	300	200	240	1800
7	3000	300	400	300	240	2200
8	3200	200	300	400	240	2200
9	3400	250	250	250	200	2400
10	3000	400	200	400	240	2000

In the following Table, the results are presented.

Table 6.2: IMU Results for Mode 0 (S-movement)

Test	ΔPitch [°]	ΔRoll [°]	ΔYaw [°]	Acc. peak [m/s^2]
1	4.44	1.82	0.87	0.324
2	5.37	0.81	4.56	0.383
3	3.06	7.87	2.19	0.363
4	2.13	3.06	3.37	0.344
5	3.81	7.06	3.88	0.346
6	3.75	3.44	2.19	0.284
7	4.50	1.32	4.43	0.275
8	3.31	5.56	1.62	0.316
9	4.05	6,43	2.54	0.289
10	4.98	5.04	1.91	0.322

The generation of a S-movement, so a curvature more similar to a wave, tends to push the body down and then brings it back up. The principal observation is on the pitch, that is directly proportional to the width (when one is increasing, the other one is

increasing too). The roll is very limited, which suggests that the wave is symmetric. The yaw presents some variations, but nothing stable or relevant.

6.3.2 Mode 1 - All the SMA

This is the mode in which all four SMA are simultaneously actuated without phase shift, so that the deformation of the fin is symmetric and it tends to produce a more compact stroke with a uniform deflection of the fin.

Table 6.3: Used parameters for each trial in Mode 1 (All the SMA)

	amp	up [ms]	hold [ms]	down [ms]	cool [ms]
1	2200	150	150	150	1200
2	2600	200	200	200	1500
3	2800	250	200	250	1600
4	3000	300	250	300	1800
5	3200	300	300	300	2200
6	3000	150	250	300	2000
7	3000	300	400	300	2600
8	3200	200	0	300	1800
9	3400	250	250	250	2800
10	2800	400	200	400	2000

Table 6.4: IMU Results for Mode 1 (All the SMA)

Test	ΔPitch [°]	ΔRoll [°]	ΔYaw [°]	Acc. peak [m/s^2]
1	4.63	2.63	1.12	0.54
2	4.57	4.75	1.12	0.51
3	4.38	3.63	1.44	0.82
4	3.81	2.12	0.94	0.42
5	2.69	2.75	0.62	0.40
6	4.06	2.81	1.07	0.53
7	5.56	3.94	1.37	0.43
8	4.31	3.57	1.68	0.38
9	4.00	3.50	0.75	0.47
10	4.69	2.12	1.51	0.63

As it is shown in the Table, there is a gradual increasing on the force, which leads to a width increment of the measured pitch on the IMU and on little variations of the yaw, mostly due to the asymmetric assembly. The roll remains at low values. The accelerations are a little bit inferior with respect to the previous movement, because this does not simulate a wave.

6.3.3 Mode 2 - TOP (only superior half)

This configuration, in which the movement is exclusively on the superior half of the fin, was chosen to study the produced imbalance upwards, studying the rotation of the body in a specific direction.

Also in this case, the condition in the beginning are softer, increasing more and more each trial.

Table 6.5: Used parameters for each trial in Mode 2 (TOP - Superior Half)

	amp	up [ms]	hold [ms]	down [ms]	cool [ms]
1	2400	150	150	150	1000
2	2600	200	200	200	1300
3	2800	250	200	250	1500
4	3000	300	250	300	1700
5	3200	300	300	300	2100
6	3000	150	250	300	1900
7	3000	300	400	300	2300
8	3200	200	0	300	1700
9	2800	400	200	400	1900
10	3000	250	250	400	1900

Table 6.6: IMU Results for Mode 2 (Superior Half)

Test	ΔPitch [°]	ΔRoll [°]	ΔYaw [°]	Acc. peak [m/s^2]
1	1.81	0.62	0.31	0.17
2	1.88	0.94	0.19	0.18
3	1.94	1.50	0.06	0.19
4	1.94	1.38	0.75	0.17
5	1.94	1.13	0.75	0.17
6	1.87	1.44	0.87	0.18
7	0.50	0.44	0.25	0.11
8	1.13	0.56	1.25	0.22
9	1.69	0.87	0.88	0.17
10	2.32	1.69	0.75	0.20

In this mode, the body is rotated downwards, the pitch grows and also the roll, because the superior part generates a torsion. The tests show also the increment of the yaw, which suggests an asymmetric flow. It is useful to study the body sensibility, not the non-symmetric forces.

6.3.4 Mode 3 - BOTTOM (only inferior half)

The final mode is the opposite of the previous one: only the inferior half is actuated, expecting to generate a rotation of the body in the opposite direction of the previous one.

Table 6.7: Used parameters for each trial in Mode 3 (BOTTOM - Inferior Half)

	amp	up [ms]	hold [ms]	down [ms]	cool [ms]
1	2400	150	150	150	1000
2	2600	200	200	200	1300
3	2800	250	200	250	1500
4	3000	300	250	300	1700
5	3200	300	300	300	2100
6	3000	150	250	300	1900
7	3000	300	400	300	2300
8	3200	200	0	300	1700
9	2800	400	200	400	1900
10	3000	250	250	400	1900

Table 6.8: IMU Results for Mode 3 (Inferior Half)

Test	ΔPitch [°]	ΔRoll [°]	ΔYaw [°]	Acc. peak [m/s^2]
1	2.62	2.56	1.13	0.21
2	3.56	2.38	0.25	0.25
3	3.37	1.94	0.37	0.22
4	3.25	2.12	0.50	0.20
5	2.63	2.75	0.31	0.21
6	2.75	2.69	0.44	0.24
7	2.00	1.81	0.44	0.24
8	2.13	2.56	0.44	0.27
9	2.31	1.69	0.81	0.19
10	3.31	3.31	0.69	0.23

As the Table shows, this mode produces the opposite effects of the previous configuration: the body rotates upwards, the oscillation of the pitch is inverted with respect the previous one, the roll is sufficiently high and the contribution of the yaw is practically null. Also this mode is more useful to study the stability, in this case of the inferior part.

6.4 Results and Discussion

In this section, the collected data are analyzed for each actuation mode. The focus of this analysis is to understand the dynamic effect of each actuation on the stability of the body, identifying differences on the behavior of the system.

In mode 0, there are moderate variation of the pitch, with values between 2.1° and 5.37°, with a gradual increasing due to the up-hold-down phase of the SMA. The roll values are stable, with variation between 0.81° and 7.87°, with significant oscillations and a lateral torsional amplification. The recorded accelerations have low values, rarely over 0.383, since the actuation phase is progressive and non-impulsive. This is a mode with a more progress movement, not a violent stroke and it introduces a lateral component,

recorded on the values of pitch and yaw. The introduction of the phase shift can cause a more complex movement during the deformation, composed of lateral asymmetries, but the force is reduced.

In mode 1, the pitch variation has a value range of 3.8° and 5.5°, remarking a rotation upwards or downwards, depending on the phase of the stroke. Also the roll variation, between 2.1° and 3.9°, shows significant oscillations and an important torsional contribution of the fin. The peak acceleration is the highest of all modes, with a maximum of 0.82. Simultaneously activating all the SMA, there is the generation of the maximum force, which leads a high inclinations. This mode confirms the capability of the fin to reproduce significant dynamic movements, maximizing the force and acceleration and increasing the instability.

In mode 2, activating only the superior half of the fin, there is a moderate contribution of the pitch variation on the vertical rotation, assuming values between 0.5° and 2.32°. The roll variation presents lower values, between 0.44° and 1,69°. The acceleration peak is the lowest of all modes, which tells a softer movement. The actuation of the superior half generates a force located only in the superior part of the fin, with a more stable system and lower rotations, confirming the partial pitch contribution.

In mode 3, the exact opposite of the mode 2, only the inferior half is activated. The pitch variation is higher than the previous one, with values of 2° and 3.56°, but it was expected considering that the lower part has more lever arm in pitching generation. The roll variation is also higher than the previous one, probably because the lower part produces an higher torsion. The peak acceleration is also higher than the previous mode. Generally, the SMA in the inferior part provides a more energetic response and the behavior remains stable with respect the previous modes, understanding that they are responsible of the vertical inclination and that this is a good compromise between force and stability.

Considering the yaw, the only relevance of this parameter is in the mode 0, with S-movement, with values between 0.87° and 4.56°, showing also horizontal rotations. For all the other modes, the behavior of the yaw is practically inconsiderable.

On a biomechanical point of view, the behavior is very similar to a real fin: the lower part is the one more involved in the pitching control, while the upper part has a stabilization role. In conclusion, the experiment shows that the system is capable of generating repeatable and adjustable movements that align with the chosen actuation strategy, confirming the efficacy of SMA-base solution.

Chapter 7

Conclusions and Future Work

7.1 Summary of Achievements

The thesis project had as main objective the modeling, realization and experimental characterization of an active biomimetic caudal fin, actuated through SMA wires, integrated in a prototype robotic fish to study the effects of the pitching stabilization.

Many results in various sectors were obtained, such as:

- the analysis of the state of the art of underwater robotic vehicles, with a particular focus on the swimming mode BCF (Body and/or Caudal Fin), on the actuation with soft materials and on the problems of the control of the SMA and stabilization of the fish body
- construction of a caudal fin, inspired mainly on the carangiform of fishes, actuated through four SMA wires, able to generate acceptable and repeatable deformations, improving the performances with respect to the previous prototype with only two SMA wires
- design of a new electronic system, based on an ESP32-S3 microcontroller, improved with respect to the old version, adding also an interface with the user and an improved data collection
- integration of an inertial sensor (IMU) BNO055, used to measure the pitch and roll of the prototype, studying the different rotations of the body caused only on the actuation of the caudal fin
- a static calibration of the fin, studying the experimental relation between the current, the resistance of the SMA and the deflection angle of the fin; this analysis leads to a design of an approximation of a linear model resistance-angle, since the low coefficient R^2 does not fully allow it

- implementation of a simplified dynamic linear model and a PID controller designed with the Ziegler-Nichols modified method, showing that the controller was able to improve the rapidity of the response and to reduce the overshoot
- experimenting the effects of the caudal fin on the pitching stabilization, testing the fin in four modes (S-movement, simultaneous actuation of all SMA, only the inferior half and only the superior half), showing that the fin can generate the pitch measurable and repeatable movements

As it can be seen, these results confirm the concept of design an actuated caudal fin through SMA, setting the foundation for future works on several fields, such as the modeling and the control, but also on the realization of a complete robotic fish for monitoring applications in marine environment.

7.2 Prototype Limitations

The obtained results in each field are quite positive, but with some limitations that cannot be neglected, but they can be an initial setting to orientate the future works.

From the mechanical point of view, the fin was designed starting from a resin mold and pouring silicone, properly fixing the SMA wires through positioning pins. This has guaranteed a good functionally, but the connection between the fin and the rigid body of the fish was obtained with raw solutions (hot glue and tape) and the rigid body was simulated with a rigid standard tube, without any concern about the mass distribution and buoyancy. Obviously, this was a laboratory experiment, so all these precautions were not taken in consideration, but maybe in an industrial use they should.

From the electrical point of view, the system is based on an ESP32-S3 board and multiple channels, showing a good reliability, but with the following limitations:

- the system is not energetically autonomous, since an external power supply is used
- the sampling frequency and the DAC resolution were appropriate for static tests, not for rapid controls and high-frequency maneuvers
- the current and voltage measurements are affected by noises and thermal variations of sensors and SMA wires

The static calibration resistance-angle has highlighted an enormous data dispersion, caused by the dependence on thermal conditions of the SMA (for example, cooling in the water). The linear model partially explains the behavior, due to the low value of the coefficient R^2, making unreliable the use of the resistance to estimate precisely the angle.

The simplification of the dynamic model, reduced to a first order transfer function, does not take in consideration the thermal hysteresis of the SMA, the saturation and

the hydrodynamics interactions between the fin and the water, which can be relevant in high-frequency applications. Consequently, the PID controller represents a not completely valid realistic model, indeed it was not implemented during experiments.

Looking at the experiments:

- the video resolution and the manual marker on the fin have affected the angle measurements on Tracker, but not a huge influence
- the pitching stabilization was conducted on a limited number of tests for each mode, and the setup of the whole system is far from the actual setup of a perfect robotic fish, which can swim freely on a tank
- the hydrodynamic forces were not measured, but only the variation of orientation

But it does not mean results were not sufficient enough, but they define a clear validity range, showing the experimental start to design more compact and robust solutions.

7.3 Future Developments

From the results and limitations explained in the chapter, there are several adjustments and additions that can be developed.

The first field to improve is the mechanical and electrical part of the prototype, making it more robust, repeatable and adaptable for longer time for tests. A few suggestions would be:

- modeling a robotic fish body specific for the application, with a more accurate mass distribution and buoyancy distribution, obtaining a more realistic hydrostatic and hydrodynamic stability
- modeling a more stable mechanical interface between fin and body, printing in 3D appropriate pieces and supports to guarantee a more simple assembling
- integrating an on-board battery system with a charging model, to make the prototype electrically independent

Other improvements can be about the modeling of the fin and the SMA actuators, which for now is based on a simplified linear model and on experimental data affected by a marked variability. Some improvements can be the following:

- continuing the experimental trials to obtain more accurate model for the thermo-mechanical behavior of the SMA wire

- designing a nonlinear electro-thermo-mechanical model, taking in consideration phenomenons such as thermal hysteresis, phase transformation, thermal history dependency, self-heating and convective cooling
- integrating a model with hydrodynamics interactions

The most significant improvement that can be done for the project is the automatic control of the fin, that is the next step for the current open-loop control. As already explained, the SMA are nonlinear actuators because the response depends on many factors, such as the temperature, the current and thermal history dependency. For this reason, the initial approach with a PID controller is not sufficient enough to obtain reliable performances on the prototype.

Studying and adopting nonlinear advanced approaches can be interesting. Some of them are:

- adaptive control: it updates the parameters of the controller in real time, depending on the system state
- sliding mode control (SMC): to use it to compare uncertainties and disturbances
- feedback linearization: it allows to obtain linear dynamics in a nonlinear application
- gain scheduling: it varies the controller gains, considering the temperature of the SMA wire or the width deflection
- nonlinear model predictive control (NMPC): it is used to optimize the behavior of the actuator, without exceeding the limits of the temperature, current and dynamic performances

In the short term, a possible evolution would be the implementation of an IMU-based closed-loop PID control, adapting the gains according to the thermal state of the actuator.

In conclusion, a promising direction to extend the work for a complete robotic fish is the integration of multiple fins (pectoral fins and dorsal fin) and to study the coordination between them. Doing this, it would be possible to evaluate some topics such as three-dimensional body stabilization, generation of complex trajectories, fine maneuverability, all of these for potential applications in underwater environmental monitoring and low-impact bio-inspired robotics.

7.4 Sustainability and UN 2030 Agenda

The study conducted could be described in a wider context, aimed at environmental sustainability and marine ecosystem preservation in line with the principles outlined in the United Nations 2030 Agenda for Sustainable Development.

Among the seventeen objectives of the Agenda, the fourteenth goal (Life Below Water, "Conserve and Sustainably use the oceans, seas, and marine resources for sustainable development") plays an important role to guarantee the future development of the planet.

Figure 7.1: Life Below Water of the UN 2030 Agenda

The 70 % of the earth surface is made of water, so it is understandable the important role of the oceans in the climatic regulation, in the production of oxygen, in the biodiversity and in the economic resources. Today, it is in danger this part of the planet is in danger, mostly due to phenomena such as pollution, acidification, global warming, and overfishing. In this context, technological innovation could be useful to monitor and protect the underwater environments.

This research, dedicated to the development of an active biomimetic caudal fin, can be seen in this way and it represents first step for the progress and realization of underwater robotic systems at low-impact and high energy efficiency. The biomimetic approach, inspired to the morphology and kinematics of the fish swimming, is able to reproduce fluid and natural movements, reducing noises and turbulences generated by the propulsion. While traditional underwater vehicles are based on rigid propellers and complex mechanical systems, in bio-inspired robots softer and more deformable structures are used, which are able to make an harmonious interaction with the environment, avoiding disturbances to the marine fauna and enhancing hydrodynamic efficiency. This characteristic is relevant for observing and monitoring the environment because these movements do not alter the normal behavior of aquatic organisms.

The integration of SMA actuators and the inertial sensor IMU allow to develop autonomous systems capable to adapt the trajectory and their structure according to the conditions of the fluid around them. These characteristics are important to make a non invasive robot for monitoring for many reasons, such as the water quality, mapping or observation of the fauna, contributing to the data collection for the safeguard of the marine environment.

Devices based on the same technologies could be integrated in sensors, distributed in networks, for environmental monitoring or for the management of protected marine areas, directly supporting Targets 14.2 and 14.5 of the UN 2030 Agenda, which promote

sustainable management of marine ecosystems and the expansion of ocean conservation zones.

Besides the direct impact on scientific researches, these robotic systems have a great potential in education and public outreach. The functioning of a real robot which replicated movements inspired from the nature and showing them to people could help to raise awareness, especially the new generation, on the relevance of ocean preservation and of the responsible use of natural resources.

The use of soft materials and energy-efficient actuators promote a new technology, which respect more the environment, adopting the basic principles of sustainability, efficiency and circular design.

In conclusion, the development of biomimetic robotic systems represents not only a progress on the field of underwater robotic, but also a demonstration of how scientific researches are directly connected to sustainability.

Through the fusion of biological and engineering knowledge, these devices allow to explore and monitor the underwater environment in a more intelligent and sustainable way, reducing ecological impact and promoting a more responsible management of aquatic ecosystems.

Bio-inspired robotic is not only a biological imitation, but a way to harmoniously connect the technological progress and the protection of oceans.

Bibliography

[1] Li, Y., Xu, Y., Wu, Z., Ma, L., Guo, M., Li, Z., and Li, Y. *A Comprehensive Review on Fish-Inspired Robots. International Journal of Advanced Robotic Systems*, vol. 19, no. 3, 2022, pp. 1–20. DOI: 10.1177/17298806221103707.

[2] Martínez-García, E. A., Lavrenov, R., and Magid, E. *Robot Fish Caudal Propulsive Mechanisms: A Mini-Review. AI, Computer Science and Robotics Technology*, 2022, pp. 1–17. DOI: 10.5772/acrt.09.

[3] Yuan, W., Hao, S., Liu, Z., Zhou, F., and Wu, Y. *Performance Analysis and Design of a Robotic Fish for In-Water Monitoring. Journal of Marine Science and Engineering*, vol. 13, 1116, 2025. DOI: 10.3390/jmse13061116.

[4] Di Santo, V., Lauder, G. V., and Nauen, J. C. *Inherent Instability Leads to High Costs of Hovering in Near-Neutrally Buoyant Fishes. Proceedings of the National Academy of Sciences (PNAS)*, 2025.

[5] Ting, S. C., and Yang, J. T. *Pitching Stabilization via Caudal Fin-Wave Propagation in a Forward-Sinking Parrot Cichlid. Journal of Experimental Biology*, vol. 211, 2008, pp. 3147–3159. DOI: 10.1242/jeb.020263.

[6] Abdulameer, A., Sulaiman, M., Aras, M. S. M., and Saleem, D. *GUI Based Control System Analysis Using PID Controller for Education. Indonesian Journal of Electrical Engineering and Computer Science*, vol. 3, no. 1, 2016, pp. 91–101. DOI: 10.11591/ijeecs.v3.i1.pages.

[7] Ma, S., Zhao, Q., Ding, M., Zhang, M., Zhao, L., Huang, C., Zhang, J., Liang, X., Yuan, J., Wang, X., and He, G. *A Review of Robotic Fish Based on Smart Materials. Biomimetics*, vol. 8, 2023, article 227. DOI: 10.3390/biomimetics8030227.

[8] Teh, Y. H., and Featherstone, R. *An Architecture for Fast and Accurate Control of Shape Memory Alloy Actuators. Proceedings of the IEEE International Conference on Robotics and Automation (ICRA)*, 2008, pp. 2021–2026. DOI: 10.1109/ROBOT.2008.4543490.